

Article

Not peer-reviewed version

Robust Multi-Performances Control for Four-Link Manipulator Arm

[Kuang-Hui Chi](#), Yung-Feng Hsiao, [Chung-Cheng Chen](#)*

Posted Date: 25 March 2025

doi: 10.20944/preprints202503.1847.v1

Keywords: Almost disturbance decoupling performance; COVID-19 prevention robotics; feedback linearized approach; four-link manipulator arm; nonlinear convergence rate



Preprints.org is a free multidisciplinary platform providing preprint service that is dedicated to making early versions of research outputs permanently available and citable. Preprints posted at Preprints.org appear in Web of Science, Crossref, Google Scholar, Scilit, Europe PMC.

Copyright: This open access article is published under a Creative Commons CC BY 4.0 license, which permit the free download, distribution, and reuse, provided that the author and preprint are cited in any reuse.

Article

Robust Multi-Performances Control for Four-Link Manipulator Arm

Kuang-Hui Chi ¹, Yung-Feng Hsiao ² and Chung-Cheng Chen ^{3,*}

¹ Department of Electrical Engineering, National Yunlin University of Science and Technology, 123 University Road, Section 3, Douliou, Yunlin 640301, Taiwan, R.O.C.

² Graduate school of engineering science and technology, National Yunlin University of Science and Technology, 123 University Road, Section 3, Douliou, Yunlin 640301, Taiwan, R.O.C.

³ Department of Electrical Engineering, National Chiayi University, 300, Syuefu Road, 60004 Chiayi City, Taiwan, R.O.C.

* Correspondence: ccc49827@ms25.hinet.net

Featured Application: Design of robust and tracking controller for four-link manipulator arm is an important subject for many industrial applications such as COVID-19 prevention robotics, agricultural mobile robotics, mining mobile robotics, space exploration mobile robotics, lower limb rehabilitation robotics, biped walking robotics and underwater robotics.

Abstract: Robust control of the four-link manipulator arm (FLMA) is an important subject for many industrial applications such as COVID-19 prevention robotics, lower limb rehabilitation robotics and underwater robotics. This study uses the feedback linearized approach to stabilize the complex nonlinear FLMA without applying nonlinear approximator that includes the fuzzy approach and the neural network optimal approach. The article proposes a new approach based on the “first” derived nonlinear convergence rate formula of FLMA to control the highly nonlinear dynamics. The linear quadratic regulator (LQR) method is often applied in the balance controlling space of the underactuated manipulator. This proposed approach takes the place of LQR approach without the necessary trial and error operations. The implications of proposed approach are “globally” valid, whereas the Jacobian linearized approach is “locally” valid. In addition, the main innovation of the proposed method is to perform “simultaneously” additional performances including the almost disturbance decoupling performance that takes the place of the traditional posture-energy approach and avoids some torque chattering behaviour in the swing-up space, and globally exponential stable performance without solving the Hamilton-Jacobi equation. Comparative examples show that the proposed controller is superior to the singular perturbation and the fuzzy approaches.

Keywords: almost disturbance decoupling performance; COVID-19 prevention robotics; feedback linearized approach; four-link manipulator arm; nonlinear convergence rate;

1. Introduction

The automation of manipulator arm has gained tremendous attention in recent decades due to their wide range of engineering applications, such as agricultural mobile robotics [1], mining mobile robotics [1], space exploration mobile robotics [2], lower limb rehabilitation robotics [3], biped walking robotics [4], unmanned ground vehicle [5] and underwater robotics [6]. There are two types of manipulator arm: underactuated one [7–9], which is a kind of a nonlinear system with fewer control inputs than degrees of freedom, and fully actuated one [5,6,10,11], which is not. In general, underactuated manipulator arms are grouped into vertical types which are controlled by gravity and planar types which are not.

For the vertical underactuated manipulator, the linear Jacobian approximated model of the inverted equilibrium position is completely controllable because the controllability matrix of the linear Jacobian approximated model is full rank. For most traditional approaches of solving the complexity of vertical underactuated manipulator, the operation space is mainly separated into a swing-up space and a balance space. In the swing-up space, the control methods include posture-energy approach [12], energy-based approach [13], direct fuzzy control approach [11], fuzzy model reference learning control approach [11], adaptive fuzzy control approach [11], and then the linear quadratic regulator (LQR) optimal method [14] is applied in the balance space. However, to be quickly captured in the swing-up space for the manipulator arm, the control needs to be built an exact combination of energy and posture, and this property is difficult to be accomplished due to the complexity of the system dynamics [9]. Moreover, some torque chattering change occurs in the swing-up space and then the energy is quickly pumped into the system [9]. In general, in order to control the nonlinear dynamics well, the disturbance decoupling and the global stability should be simultaneously required [15]. To achieve these requirements, some significant approaches, such as model predictive control [16], deep reinforcement learning [17], multi-objective control [18], backstepping control [19] and preview control [20], have been adopted for complex nonlinear systems. However, in the aforementioned approaches, a serious common drawback is that the considered nonlinear systems should be approximated to be linear dynamics by the Taylor expansion for small effect operating range. This serious drawback may be impractical for the FLMA. To solve nonlinear serious drawback of the FLMA, nonlinear function approximators, such as neural network optimal approach [21] and famous fuzzy method [22], have been adopted to reduce the caused errors [23]. The main drawback of famous fuzzy method is that constructing fuzzy rule base needs to rely on many past accumulated knowledges, and then the system performance is almost determined by the constructed experience rule base [24]. The neural network optimal approach is an intelligent supervised learning approach that requires the operating network to offer many sample points [25]. The performance of controller design for the neural network method is completely limited by only applying the current state value. Moreover, complicated interconnecting structure and digital computing loads let the physical realization of nonlinear function approximators be impractical. LQR is a common method that calculates the weighting matrices Q and R for a Jacobian linearized system via trial and error operation. Some improved approaches of calculating the weighting matrices, such as genetic algorithm approach and Kalman's pole-assignment approach, have been proposed in recent decades. However, their main serious drawbacks including high computing effort and slowly convergent rate of globally optimal solution limit their performances [26].

On the other hand, planar underactuated manipulator is not constrained by gravity, so any position of the manipulator arm is the equilibrium point and the linear Jacobian approximated model at any equilibrium point is uncontrollable [27]. The control approaches for the vertical underactuated manipulator cannot be applied for planar underactuated manipulator. The researches of controlling planar underactuated manipulator are extensive and some important methods, such as the nilpotent approximated method [28], the converting-chained form method [29] and the order-reduction method [30], have been proposed to perform the position control for planar underactuated manipulator. However, the aforementioned approaches of controlling the planar underactuated manipulator are only valid for the nominal plant model. In real systems, nonlinear acting factors need to be considered [31] and then aforementioned approaches cannot be applied for the practical planar underactuated manipulator.

So far, it is obvious to see that the robust and tracking controller design for manipulator arm still is a challenging subject due to the strict global stability requirement and disturbances reduction involving on the nonlinear system dynamics. Stimulated by these points, we apply feedback linearized approach to construct the robust and tracking controller of manipulator arm with the almost disturbance decoupling, adjustable convergence rate and "globally" exponentially stable performances and take the place of "locally" Jacobian linearized method. Feedback linearized approach have contributed many significant researches [32–36] in industrial applications, such as the

dual parallel-PMSM system [32], the grid-tied packed e-cell inverter [33], PHEVs charging station [34], artificial pancreas [35] and the weak AC grid integration [36].

References [37,38] had exploited the fact that the stricter tracking error condition of almost disturbance decoupling performance including absolute error, integral error and input-to-state-stable error is involved to reduce the disturbance effect. However, they can only achieve the almost disturbance decoupling performance of nonlinear system without the nonlinearity multiplied with disturbance requirement and the non-Lipschitz nonlinearity requirement. Therefore, the almost disturbance decoupling performance cannot be achieved for the following nonlinear system: $\dot{x}_1(t) = \tan^{-1}(x_2) + w_{noise}(t)$, $\dot{x}_2(t) = u_{fb}$, $y_{o1} = x_1 \equiv \sigma_{o1}$, where σ_{o1} and u_{fb} are the output and control input, respectively. On the contrary, the almost disturbance decoupling performance can be well achieved by the proposed method. The main novelty of this study is to design robust and tracking controller for nonlinear complex FLMA. Major contributions of this study are summarized as follows:

- (i) This study has “first” presented the convergence rate formula of the nonlinear FLMA.
- (ii) The FLMA is first designed by applying the feedback linearized approach with the almost disturbance decoupling performance that takes the place of the traditional posture-energy approach and avoids some torque chattering change behaviour in the swing-up space. Moreover, the proposed approach takes the place of LQR approach without the necessary trial and error operations.
- (iii) A robust and tracking controller is presented to possess the global exponential stability without solving the Hamilton-Jacobi equation that requires to be solved for the famous H-infinity approach.
- (iv) The study has proposed a new approach to improve the shortcoming of traditional fuzzy function approximators without many design experiences and knowledges.
- (v) The implications of this proposed method are “globally” valid, whereas the Jacobian linearized approach is “locally” valid.

2. Complete Mathematical Model for Four-link Manipulator Arm

The FLMA is a great platform for industrial mechanics as it is highly nonlinear control system with disturbances. In this section, we will apply Euler-Lagrange equation to derive the dynamic equations of the FLMA shown in Figure 1.

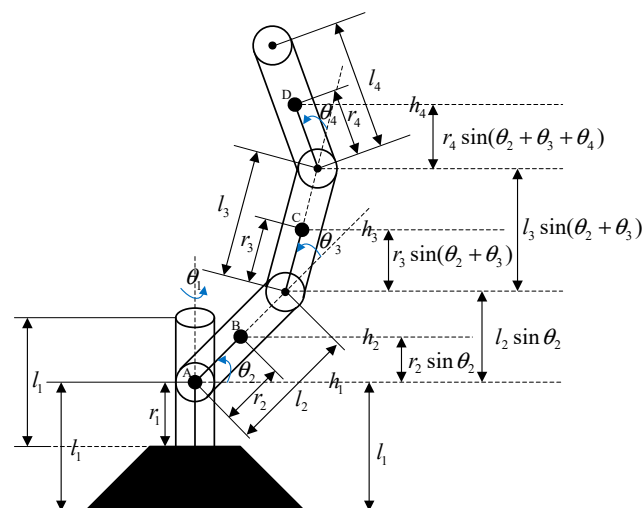


Figure 1. The four-link manipulator robot arm.

Four-link manipulator arm is made up of aluminum. The dynamic model parameters are selected as follows: the length of link $l_1 = l_2 = l_3 = l_4 = 1m$, the distance for the center of mass $r_1 = r_2 = r_3 = r_4 = 0.25m$, the mass of link $m_1 = m_2 = m_3 = m_4 = 1kg$ and the inertia moment of link $I_1 = I_2 = I_3 = I_4 = 1kg \cdot m^2$. Defining the potential energy E_p , the kinetic energy E_k , the joint torque $\bar{\tau}$, the

Lagrangian term L as the difference between the kinetic energy and potential energy, and applying the Euler–Lagrange equation yield the dynamic equation of the FLMA to be

$$L = E_K - E_P \quad (1)$$

$$\frac{d}{dt} \left(\frac{\partial L}{\partial \dot{\theta}} \right) - \left(\frac{\partial L}{\partial \theta} \right) = \bar{\tau} \quad (2)$$

$$\bar{\theta} \equiv [\theta_1 \quad \theta_2 \quad \theta_3 \quad \theta_4]^T \quad (3)$$

$$\bar{\tau} \equiv [\tau_1 \quad \tau_2 \quad \tau_3 \quad \tau_4]^T \quad (4)$$

Let the centroid translational position vector and velocity vector of link i be \bar{P}_{c_i} and \bar{v}_{c_i} , and centroid rotational position vector and velocity vector of link i be \bar{Q}_{c_i} and $\bar{\omega}_{c_i}$. From the fundamental definitions of position vector and velocity vector, we get

$$\bar{v}_{c_i} \equiv \frac{d\bar{P}_{c_i}}{dt} = \frac{\partial \bar{P}_{c_i}}{\partial \bar{\theta}} \cdot \frac{d\bar{\theta}}{dt} \equiv J_{v_i} \cdot \frac{d\bar{\theta}}{dt} = J_{v_i} \cdot \dot{\bar{\theta}} \quad (5)$$

$$J_{v_i} \equiv \frac{\partial \bar{P}_{c_i}}{\partial \bar{\theta}} \quad (6)$$

$$\bar{\omega}_{c_i} \equiv \frac{d\bar{Q}_{c_i}}{dt} = \frac{\partial \bar{Q}_{c_i}}{\partial \bar{\theta}} \cdot \frac{d\bar{\theta}}{dt} \equiv J_{\omega_i} \cdot \frac{d\bar{\theta}}{dt} = J_{\omega_i} \cdot \dot{\bar{\theta}} \quad (7)$$

and

$$J_{\omega_i} \equiv \frac{\partial \bar{Q}_{c_i}}{\partial \bar{\theta}} \quad (8)$$

Then the kinetic energy E_K of the manipulator arm will be given by

$$\begin{aligned} E_K &= \frac{1}{2} \sum_{i=1}^4 m_i \bar{v}_{c_i}^T \bar{v}_{c_i} + \frac{1}{2} \sum_{i=1}^4 m_i \bar{\omega}_{c_i}^T I_i \bar{\omega}_{c_i} \\ &= \frac{1}{2} \sum_{i=1}^4 m_i \dot{\bar{\theta}}^T (J_{v_i}^T J_{v_i}) \dot{\bar{\theta}} + \frac{1}{2} \sum_{i=1}^4 \dot{\bar{\theta}}^T (J_{\omega_i}^T I_i J_{\omega_i}) \dot{\bar{\theta}} \\ &= \frac{1}{2} \dot{\bar{\theta}}^T \left(\sum_{i=1}^4 (m_i J_{v_i}^T J_{v_i} + J_{\omega_i}^T I_i J_{\omega_i}) \right) \dot{\bar{\theta}} \end{aligned} \quad (9)$$

Define

$$E_{Kv} \equiv \frac{1}{2} \sum_{i=1}^4 m_i \dot{\bar{\theta}}^T (J_{v_i}^T J_{v_i}) \dot{\bar{\theta}} \quad (10)$$

$$E_{K\omega} \equiv \frac{1}{2} \sum_{i=1}^4 \dot{\bar{\theta}}^T (J_{\omega_i}^T I_i J_{\omega_i}) \dot{\bar{\theta}} \quad (11)$$

$$D \equiv \sum_{i=1}^4 (m_i J_{v_i}^T J_{v_i} + J_{\omega_i}^T I_i J_{\omega_i}) \quad (12)$$

Substituting (10)~(12) to (9) obtains

$$E_K = E_{Kv} + E_{K\omega} = \frac{1}{2} \dot{\bar{\theta}}^T D \dot{\bar{\theta}} > 0 \quad (13)$$

From (1)(2) and (13), we get

$$\frac{d}{dt} \left[\frac{\partial}{\partial \dot{\theta}} \left(\frac{1}{2} \dot{\theta}^T D \dot{\theta} \right) \right] - \frac{\partial E_K}{\partial \theta} + \frac{\partial E_P}{\partial \theta} = \bar{\tau} \quad (14)$$

Then

$$\frac{d}{dt} \left[\frac{1}{2} (D + D^T) \dot{\theta} \right] - \frac{\partial E_K}{\partial \theta} + \frac{\partial E_P}{\partial \theta} = \bar{\tau} \quad (15)$$

Since the matrix D possesses positive definite property and $D = D^T$, we get

$$D \ddot{\theta} + \dot{D} \dot{\theta} - \frac{\partial}{\partial \theta} \left(\frac{1}{2} \dot{\theta}^T D \dot{\theta} \right) + \frac{\partial E_P}{\partial \theta} = \bar{\tau} \quad (16)$$

i.e.

$$D \ddot{\theta} + \left[\dot{D} - \frac{1}{2} \frac{\partial}{\partial \theta} \dot{\theta}^T D \right] \dot{\theta} + \frac{\partial E_P}{\partial \theta} = \bar{\tau} \quad (17)$$

Define

$$C \equiv \dot{D} - \frac{1}{2} \frac{\partial}{\partial \theta} \dot{\theta}^T D \quad (18)$$

and

$$\bar{g} \equiv \frac{\partial E_P}{\partial \theta} \equiv [g_1 \quad g_2 \quad g_3 \quad g_4]^T \quad (19)$$

From (17)-(19), it is more practical to rewrite the Euler-Lagrange equation of the manipulator arm in more compact form for control purpose as follows:

$$D \ddot{\theta} + C \dot{\theta} + \bar{g} = \bar{\tau} \quad (20)$$

where \bar{g} is the vector of gravity force, C denotes the Coriolis matrix of the manipulator arm. Observing the structure of (19) obtains

$$C_{ij} = \sum_{1 \leq k \leq 4} \Gamma_{kji} \dot{\theta}_k \quad (21)$$

where

$$\Gamma_{kji} = \frac{\partial D_{ij}}{\partial \theta_k} - \frac{1}{2} \frac{\partial D_{kj}}{\partial \theta_i} \quad (22)$$

Define

$$J_i \equiv \begin{bmatrix} J_{v_i} \\ J_{\omega_i} \end{bmatrix} \quad (23)$$

and

$$M_i \equiv \begin{bmatrix} m_i & 0 & 0 & 0 & 0 & 0 \\ 0 & m_i & 0 & 0 & 0 & 0 \\ 0 & 0 & m_i & 0 & 0 & 0 \\ 0 & 0 & 0 & I_{x_i} & 0 & 0 \\ 0 & 0 & 0 & 0 & I_{y_i} & 0 \\ 0 & 0 & 0 & 0 & 0 & I_{z_i} \end{bmatrix} \quad (24)$$

Then (12) can be rewritten to be

$$D \equiv \sum_{i=1}^4 J_i^T M_i J_i \quad (25)$$

Observing Figure 1 yields the centroid translational position vector to be $\bar{P}_{c1} = [0 \ 0 \ l_1]^T$, $\bar{P}_{c2} = [r_2 c_2 c_1 \ r_2 c_2 s_1 \ r_2 s_2]^T$, $\bar{P}_{c3} = [l_2 c_2 c_1 + r_3 c_{23} c_1 \ l_2 c_2 s_1 + r_3 c_{23} s_1 \ l_1 + l_2 s_2 + r_3 s_{23}]^T$ and

$$\bar{P}_{c4} = \begin{bmatrix} l_2 c_2 c_1 + l_3 c_{23} c_1 + r_4 c_{234} c_1 \\ l_2 c_2 s_1 + l_3 c_{23} s_1 + r_4 c_{234} s_1 \\ l_2 s_2 + l_3 s_{23} + r_4 s_{234} + l_1 \end{bmatrix} \quad (26)$$

where $c_i \equiv \cos \theta_i$ and $s_i \equiv \sin \theta_i$. $c_{ijk} \equiv \cos(\theta_i + \theta_j + \theta_k)$, $s_{ijk} \equiv \sin(\theta_i + \theta_j + \theta_k)$, $c_{ij} \equiv \cos(\theta_i + \theta_j)$, $s_{ij} \equiv \sin(\theta_i + \theta_j)$.

Applying (6) to the centroid translational position vector gets

$$J_{v_1} = \begin{bmatrix} 0 & 0 & 0 & 0 \\ 0 & 0 & 0 & 0 \\ 0 & 0 & 0 & 0 \end{bmatrix} \quad (27)$$

$$J_{v_2} = \begin{bmatrix} -r_2 c_2 s_1 & -r_2 s_2 c_1 & 0 & 0 \\ r_2 c_2 c_1 & -r_2 s_2 s_1 & 0 & 0 \\ 0 & r_2 c_2 & 0 & 0 \end{bmatrix} \quad (28)$$

$$J_{v_3} = \begin{bmatrix} -l_2 c_2 s_1 - r_3 c_{23} s_1 & -l_2 s_2 c_1 - r_3 s_{23} c_1 & -r_3 s_{23} c_1 & 0 \\ l_2 c_2 c_1 + r_3 c_{23} c_1 & -l_2 s_2 s_1 - r_3 s_{23} s_1 & -r_3 s_{23} s_1 & 0 \\ 0 & l_2 c_2 + r_3 c_{23} & r_3 c_{23} & 0 \end{bmatrix} \quad (29)$$

$$J_{v_4} = \begin{bmatrix} -l_2 c_2 s_1 - l_3 c_{23} s_1 - r_4 c_{234} s_1 & -l_2 s_2 c_1 - l_3 s_{23} c_1 - r_4 s_{234} c_1 & -l_3 s_{23} c_1 - r_4 s_{234} c_1 & -r_4 s_{234} c_1 \\ l_2 c_2 c_1 + l_3 c_{23} c_1 + r_4 c_{234} c_1 & -l_2 s_2 s_1 - l_3 s_{23} s_1 - r_4 s_{234} s_1 & -l_3 s_{23} s_1 - r_4 s_{234} s_1 & -r_4 s_{234} s_1 \\ 0 & l_2 c_2 + l_3 c_{23} + r_4 c_{234} + l_1 & l_3 c_{23} + r_4 c_{234} & r_4 c_{234} \end{bmatrix} \quad (30)$$

Observing Figure 1 yields the centroid rotational position vector to be $\bar{Q}_{c1} = [0 \ 0 \ \theta_1]^T$, $\bar{Q}_{c2} = [0 \ \theta_2 \ \theta_1]^T$, $\bar{Q}_{c3} = [0 \ \theta_2 + \theta_3 \ \theta_1]^T$ and $\bar{Q}_{c4} = [0 \ \theta_2 + \theta_3 + \theta_4 \ \theta_1]^T$. Using (8) to the centroid rotational position vector obtains

$$J_{\omega_1} = \begin{bmatrix} 0 & 0 & 0 & 0 \\ 0 & 0 & 0 & 0 \\ 1 & 0 & 0 & 0 \end{bmatrix} \quad (31)$$

$$J_{\omega_2} = \begin{bmatrix} 0 & 0 & 0 & 0 \\ 0 & 1 & 0 & 0 \\ 1 & 0 & 0 & 0 \end{bmatrix} \quad (32)$$

$$J_{\omega_3} = \begin{bmatrix} 0 & 0 & 0 & 0 \\ 0 & 1 & 1 & 0 \\ 1 & 0 & 0 & 0 \end{bmatrix} \quad (33)$$

$$J_{\omega_4} = \begin{bmatrix} 0 & 0 & 0 & 0 \\ 0 & 1 & 1 & 1 \\ 1 & 0 & 0 & 0 \end{bmatrix} \quad (34)$$

Substituting (24)~(25) and (27)~(34) to (25) yields the matrix D as

$$\tilde{D} = \begin{bmatrix} D_{11} & 0 & 0 & 0 \\ 0 & D_{22} & D_{23} & D_{24} \\ 0 & D_{23} & D_{33} & D_{34} \\ 0 & D_{24} & D_{34} & D_{44} \end{bmatrix} \quad (35)$$

where

$$D_{11} = I_{z_1} + I_{z_2} + I_{z_3} + I_{z_4} + m_2 r_2^2 c_2^2 + m_3 l_2^2 c_2^2 + 2m_3 l_2 r_3 c_2 c_{23} + m_3 r_3^2 c_{23}^2 + m_4 l_2^2 c_2^2 + 2m_4 l_2 l_3 c_2 c_{23} + 2m_4 l_2 r_4 c_2 c_{234} + m_4 l_3^2 c_{23}^2 + 2m_4 l_3 r_4 c_{23} c_{234} \quad (36)$$

$$D_{22} = I_{y_2} + I_{y_3} + I_{y_4} + m_2 r_2^2 + m_3 l_2^2 + m_2 r_3^2 + 2m_3 l_2 r_3 c_3 + m_4 l_2^2 s_2^2 c_1^2 + 2m_4 l_2 l_3 s_2 s_{23} c_1^2 + m_4 l_3^2 s_{23}^2 c_1^2 + 2m_4 l_3 r_4 s_{23} s_{234} c_1^2 + 2m_4 l_2 r_4 s_2 s_{234} c_1^2 + m_4 r_4^2 s_{234}^2 c_1^2 \quad (37)$$

$$D_{23} = I_{y_3} + I_{y_4} + m_3 l_2 r_3 c_3 + m_4 l_2 l_3 c_3 + m_4 l_2 r_4 c_{34} + 2m_4 l_3 r_4 c_4 + m_3 r_3^2 + m_4 l_3^2 + m_4 r_4^2 \quad (38)$$

$$D_{24} = I_{y_4} + m_4 l_2 r_4 c_{34} + m_4 l_3 r_4 c_4 + m_4 r_4^2 \quad (39)$$

$$D_{33} = I_{y_3} + I_{y_4} + m_3 r_3^2 + m_4 l_3^2 + 2m_4 l_3 r_4 c_4 + m_4 r_4^2 \quad (40)$$

$$D_{34} = I_{y_4} + m_4 l_3 r_4 c_4 + m_4 r_4^2 \quad (41)$$

$$D_{44} = I_{y_4} + m_4 r_4^2 \quad (42)$$

Let us combine (21) and (22) and get the matrix \tilde{C} as

$$\tilde{C} = \begin{bmatrix} C_{11} & C_{12} & 0 & 0 \\ C_{21} & C_{22} & C_{23} & C_{24} \\ C_{31} & C_{32} & C_{33} & C_{34} \\ C_{41} & C_{42} & C_{43} & C_{44} \end{bmatrix} \quad (43)$$

where

$$C_{11} = \{m_2 r_2^2 \sin(2\theta_2) - m_3 l_2^2 \sin(2\theta_2) - 2m_3 l_2 r_3 \sin(2\theta_2 + \theta_3) - m_3 r_3^2 \sin(2\theta_2 + 2\theta_3) - m_4 l_2^2 \sin(2\theta_2) - 2m_4 l_2 l_3 \sin(2\theta_2 + \theta_3) - 2m_4 l_2 r_4 \sin(2\theta_2 + 2\theta_3 + \theta_4) - m_4 l_3^2 \sin(2\theta_2 + 2\theta_3) - 2m_4 l_3 r_4 \sin(2\theta_2 + 1\theta_3 + \theta_4) - m_4 r_4^2 \sin(2\theta_2 + 2\theta_3 + 2\theta_4)\} \dot{\theta}_2 + \{-2m_3 l_2 r_3 s_{23} c_2 - 2m_3 r_3^2 s_{23} c_{23} - 2m_4 l_2 l_3 s_{23} c_2 - 2m_4 l_2 r_4 s_{234} c_2 - 2m_4 l_3^2 s_{23} c_{23} - 2m_4 l_3 r_4 s_{234} c_{23} - 2m_4 r_4^2 s_{234} c_{234}\} \dot{\theta}_3 + \{-2m_4 l_2 r_4 s_{234} c_2 - 2m_4 l_3 r_4 s_{234} c_{23} - 2m_4 r_4^2 s_{234} c_{234}\} \dot{\theta}_4 \quad (44)$$

$$C_{12} = \{m_4 l_2^2 s_1 s_2^2 c_1 + 2m_4 l_2 l_3 s_1 s_2 s_{23} c_1 + m_4 l_3^2 s_1 s_{23}^2 c_1 + 2m_4 l_3 r_4 s_1 s_{23} s_{234} c_1 + 2m_4 l_2 r_4 s_1 s_2 s_{234} c_1 + m_4 r_4^2 s_1 s_{234}^2 c_1\} \dot{\theta}_2 \quad (45)$$

$$C_{21} = \{m_2 r_2^2 s_2 c_2 + m_3 l_2^2 s_2 c_2 + m_3 l_2 r_3 s_{23} c_2 + m_3 l_2 r_3 s_2 c_{23} + m_3 r_3^2 s_{23} c_{23} + m_4 l_2^2 s_2 c_2 + m_4 l_2 l_3 s_2 c_{23} + m_4 l_2 l_3 s_2 c_{23} + m_4 l_2 r_4 s_{234} c_2 + m_4 l_2 r_4 s_2 c_{234} + m_4 l_3^2 s_2 c_{23} + m_4 l_3 r_4 s_{234} c_{23} + m_4 l_3 r_4 s_2 c_{234} + m_4 r_4^2 s_{234} c_{234}\} \dot{\theta}_1 \quad (46)$$

$$\begin{aligned}
C_{22} = & \{-2m_4l_2^2s_1s_2^2c_1 - 4m_4l_2l_3s_1s_2s_{23}c_1 - 2m_4l_3^2s_1s_2^2c_1 \\
& - 4m_4l_3r_4s_1s_{23}c_1 - 4m_4l_2r_4s_1s_{23}c_1 - 2m_4r_4^2s_1^2s_{23}c_1\}\dot{\theta}_1 + \\
& \{m_4l_2^2s_2c_1^2c_2 + m_4l_2l_3s_2c_1^2c_{23} + m_4l_2l_3s_{23}c_1^2c_2 + m_4l_3^2s_{23}c_1^2c_{23} + \\
& m_4l_3r_4s_{23}c_1^2c_{234} + m_4l_3r_4s_{234}c_1^2c_{23} + m_4l_2r_4s_2c_1^2c_{234} + m_4l_2r_4s_{234}c_1^2c_2 \\
& + m_4r_4^2s_{234}c_1^2c_{234}\}\dot{\theta}_2 + \{-2m_3l_2r_3s_3 + 2m_4l_2l_3s_2c_1^2c_{23} + 2m_4l_3^2s_{23}c_1^2c_{23} \\
& + 2m_4l_3r_4s_{23}c_1^2c_{234} + 2m_4l_3r_4s_{234}c_1^2c_{23} + 2m_4l_2r_4s_2c_1^2c_{234} + 2m_4r_4^2s_{234}c_1^2c_{234}\}\dot{\theta}_3 \\
& + \{2m_4l_3r_4s_{23}c_1^2c_{234} + 2m_4l_2r_4s_2c_1^2c_{234} + 2m_4r_4^2s_{234}c_1^2c_{234}\}\dot{\theta}_4
\end{aligned} \tag{47}$$

$$C_{23} = \{-m_3l_2r_3s_3 - m_4l_2l_3s_3 - m_4l_2r_4s_{34}\}\dot{\theta}_3 + \{-m_4l_2r_4s_{34} - 2m_4l_3r_4s_{34}\}\dot{\theta}_4 \tag{48}$$

$$C_{24} = \{-m_4l_2r_4s_{34}\}\dot{\theta}_3 + \{-m_4l_2r_4s_{34} - m_4l_3r_4s_{34}\}\dot{\theta}_4 \tag{49}$$

$$\begin{aligned}
C_{31} = & \{m_4l_2r_3s_{23}c_2 + m_3r_3^2s_{23}c_{23} + m_4l_2l_3s_{23}c_2 + m_4l_2r_4s_{234}c_2 \\
& + m_4l_3^2s_{23}c_{23} + m_4l_3r_4s_{234}c_{23} + m_4l_3r_4s_{23}c_{234} + m_4r_4^2s_{234}c_{234}\}\dot{\theta}_1
\end{aligned} \tag{50}$$

$$\begin{aligned}
C_{32} = & \{m_3l_2r_3s_3 - m_4l_2l_3s_2c_1^2c_{23} - m_4l_3^2s_{23}c_1^2c_{23} - m_4l_3r_4s_{23}c_1^2c_{234} \\
& - m_4l_3r_4s_{234}c_1^2c_{23} - m_4l_2r_4s_2c_1^2c_{234} - m_4r_4^2s_{234}c_1^2c_{234}\}\dot{\theta}_2 + \{-\frac{1}{2}m_3l_2r_3s_3 \\
& - \frac{1}{2}m_4l_2l_3s_3 - \frac{1}{2}m_4l_2r_4s_{34}\}\dot{\theta}_3 + \{-m_4l_2r_4s_{34} - 2m_4l_3r_4s_{34} + \frac{1}{2}m_4l_2r_4s_{34}\}\dot{\theta}_4
\end{aligned} \tag{51}$$

$$C_{33} = \{\frac{1}{2}m_3l_2r_3s_3 + \frac{1}{2}m_4l_2l_3s_3 + \frac{1}{2}m_4l_2r_4s_{34}\}\dot{\theta}_2 + \{-2m_4l_3r_4s_{34}\}\dot{\theta}_4 \tag{52}$$

$$C_{34} = \{\frac{1}{2}m_4l_2r_4s_{34}\}\dot{\theta}_2 + \{-m_4l_3r_4s_{34}\}\dot{\theta}_4 \tag{53}$$

$$C_{41} = \{m_4l_2r_4s_{234}c_2 + m_4l_3r_4s_{234}c_{23} + m_4r_4^2s_{234}c_{234}\}\dot{\theta}_1 \tag{54}$$

$$\begin{aligned}
C_{42} = & \{-m_4l_3r_4s_{23}c_1^2c_{234} - m_4l_2r_4s_2c_1^2c_{234} - m_4r_4^2s_{234}c_1^2c_{234}\}\dot{\theta}_2 \\
& + \{m_4l_2r_4s_{34} + \frac{1}{2}m_4l_2r_4s_{34} + m_4l_3r_4s_{34}\}\dot{\theta}_3 + \{-\frac{1}{2}m_4l_2r_4s_{34} - \frac{1}{2}m_4l_3r_4s_{34}\}\dot{\theta}_4
\end{aligned} \tag{55}$$

$$C_{43} = \{\frac{1}{2}m_4l_2r_4s_{34} + m_4l_3r_4s_{34}\}\dot{\theta}_2 + \{m_4l_3r_4s_{34}\}\dot{\theta}_3 + \{-\frac{1}{2}m_4l_3r_4s_{34}\}\dot{\theta}_4 \tag{56}$$

$$C_{44} = \{\frac{1}{2}m_4l_2r_4s_{34} + \frac{1}{2}m_4l_3r_4s_{34}\}\dot{\theta}_2 + \{\frac{1}{2}m_4l_3r_4s_{34}\}\dot{\theta}_3 \tag{57}$$

From Figure 1, we get the potential energy of manipulator arm as

$$\begin{aligned}
E_p = & gm_1l_1 + gm_2(l_1 + r_2s_2) + gm_3(l_1 + l_2s_2 + r_3s_{23}) \\
& + gm_4(l_1 + l_2s_2 + l_3s_{23} + r_4s_{234})
\end{aligned} \tag{58}$$

where $g = 9.8 \text{ Nt/kg}$. Applying (19) gets

$$g_1 = 0 \tag{59}$$

$$g_2 = gm_2r_2c_2 + gm_3l_2c_2 + gm_3r_3c_{23} + gm_4l_2c_2 + gm_4l_3c_{23} + gm_4r_4c_{234} \tag{60}$$

$$g_3 = gm_3r_3c_{23} + gm_4l_3c_{23} + gm_4r_4c_{234} \tag{61}$$

$$g_4 = gm_4r_4c_{234} \tag{62}$$

Using (35) yields the inverse of the matrix D to be

$$\tilde{D}^{-1} = \begin{bmatrix} I_{11} & 0 & 0 & 0 \\ 0 & I_{22} & I_{23} & I_{24} \\ 0 & I_{23} & I_{33} & I_{34} \\ 0 & I_{24} & I_{34} & I_{44} \end{bmatrix} \quad (63)$$

where

$$\Delta_1 \equiv D_{22}D_{33}D_{44} - D_{22}D_{34}^2 - D_{23}^2D_{44} + 2D_{23}D_{24}D_{34} - D_{24}^2D_{33} \quad (64)$$

$$I_{11} = \frac{1}{\Delta_1} \quad (65)$$

$$I_{22} = \frac{D_{33}D_{44} - D_{34}^2}{\Delta_1} \quad (66)$$

$$I_{23} = \frac{-D_{23}D_{44} + D_{24}D_{34}}{\Delta_1} \quad (67)$$

$$I_{24} = \frac{D_{23}D_{34} - D_{24}D_{33}}{\Delta_1} \quad (68)$$

$$I_{33} = \frac{D_{22}D_{44} - D_{24}^2}{\Delta_1} \quad (69)$$

$$I_{34} = \frac{-D_{22}D_{34} + D_{23}D_{24}}{\Delta_1} \quad (70)$$

$$I_{44} = \frac{D_{22}D_{33} - D_{23}^2}{\Delta_1} \quad (71)$$

From (43) and (63), we get

$$\tilde{D}^{-1}C = \begin{bmatrix} I_{11} & 0 & 0 & 0 \\ 0 & I_{22} & I_{23} & I_{24} \\ 0 & I_{23} & I_{33} & I_{34} \\ 0 & I_{24} & I_{34} & I_{44} \end{bmatrix} \begin{bmatrix} C_{11} & C_{12} & 0 & 0 \\ C_{21} & C_{22} & C_{23} & C_{24} \\ C_{31} & C_{32} & C_{33} & C_{34} \\ C_{41} & C_{42} & C_{43} & C_{44} \end{bmatrix} \equiv \begin{bmatrix} D_{c11} & D_{c12} & 0 & 0 \\ D_{c21} & D_{c22} & D_{c23} & D_{c24} \\ D_{c31} & D_{c32} & D_{c33} & D_{c34} \\ D_{c41} & D_{c42} & D_{c43} & D_{c44} \end{bmatrix} \quad (72)$$

where

$$D_{c11} = I_{11}C_{11} \quad (73)$$

$$D_{c21} = I_{22}C_{21} + I_{23}C_{31} + I_{24}C_{41} \quad (74)$$

$$D_{c31} = I_{23}C_{21} + I_{33}C_{31} + I_{34}C_{41} \quad (75)$$

$$D_{c41} = I_{24}C_{21} + I_{34}C_{31} + I_{44}C_{41} \quad (76)$$

$$D_{c12} = I_{11}C_{12} \quad (77)$$

$$D_{c22} = I_{22}C_{22} + I_{23}C_{32} + I_{24}C_{42} \quad (78)$$

$$D_{c32} = I_{23}C_{22} + I_{33}C_{32} + I_{34}C_{42} \quad (79)$$

$$D_{c42} = I_{24}C_{22} + I_{34}C_{32} + I_{44}C_{42} \quad (80)$$

$$D_{c23} = I_{22}C_{23} + I_{23}C_{33} + I_{24}C_{43} \quad (81)$$

$$D_{c33} = I_{23}C_{23} + I_{33}C_{33} + I_{34}C_{43} \quad (82)$$

$$D_{c43} = I_{24}C_{23} + I_{34}C_{33} + I_{44}C_{43} \quad (83)$$

$$D_{c24} = I_{22}C_{24} + I_{23}C_{34} + I_{24}C_{44} \quad (84)$$

$$D_{c34} = I_{23}C_{24} + I_{33}C_{34} + I_{34}C_{44} \quad (85)$$

$$D_{c44} = I_{24}C_{24} + I_{34}C_{34} + I_{44}C_{44} \quad (86)$$

Multiplying (63) with (19) yields

$$\underline{D}^{-1}\underline{\bar{g}} = \begin{bmatrix} I_{11} & 0 & 0 & 0 \\ 0 & I_{22} & I_{23} & I_{24} \\ 0 & I_{23} & I_{33} & I_{34} \\ 0 & I_{24} & I_{34} & I_{44} \end{bmatrix} \begin{bmatrix} \underline{g}_1 \\ \underline{g}_2 \\ \underline{g}_3 \\ \underline{g}_4 \end{bmatrix} \equiv \begin{bmatrix} D_{g1} \\ D_{g2} \\ D_{g3} \\ D_{g4} \end{bmatrix} \quad (87)$$

where

$$D_{g1} = I_{11} \quad (88)$$

$$D_{g2} = I_{22}g_2 + I_{23}g_3 + I_{24}g_4 \quad (89)$$

$$D_{g3} = I_{23}g_2 + I_{33}g_3 + I_{34}g_4 \quad (90)$$

$$D_{g4} = I_{24}g_2 + I_{34}g_3 + I_{44}g_4 \quad (91)$$

From (20), we obtain

$$\ddot{\underline{\theta}} = -\underline{D}^{-1}\underline{C}\dot{\underline{\theta}} - \underline{D}^{-1}\underline{\bar{g}} + \underline{D}^{-1}\underline{\bar{\tau}} \quad (92)$$

Substituting (63), (72) and (87) to (92) gets

$$\ddot{\theta}_1 = -D_{c11}\dot{\theta}_1 - D_{c12}\dot{\theta}_2 - D_{g1} + I_{11}\tau_1 \quad (93)$$

$$\ddot{\theta}_2 = -D_{c21}\dot{\theta}_1 - D_{c22}\dot{\theta}_2 - D_{c23}\dot{\theta}_3 - D_{c24}\dot{\theta}_4 - D_{g2} + I_{22}\tau_2 + I_{23}\tau_3 + I_{24}\tau_4 \quad (94)$$

$$\ddot{\theta}_3 = -D_{c31}\dot{\theta}_1 - D_{c32}\dot{\theta}_2 - D_{c33}\dot{\theta}_3 - D_{c34}\dot{\theta}_4 - D_{g3} + I_{23}\tau_2 + I_{33}\tau_3 + I_{34}\tau_4 \quad (95)$$

$$\ddot{\theta}_4 = -D_{c41}\dot{\theta}_1 - D_{c42}\dot{\theta}_2 - D_{c43}\dot{\theta}_3 - D_{c44}\dot{\theta}_4 - D_{g4} + I_{24}\tau_2 + I_{34}\tau_3 + I_{44}\tau_4 \quad (96)$$

Define the state, input and noise variables of the FLMA to be the following physical quantities:

$$\bar{x} \equiv [x_1 \ x_2 \ x_3 \ x_4 \ x_5 \ x_6 \ x_7 \ x_8]^T, \ x_1 = \theta_1, \ x_2 = \dot{\theta}_1, \ x_3 = \theta_2, \ x_4 = \dot{\theta}_2, \ x_5 = \theta_3, \ x_6 = \dot{\theta}_3, \ x_7 = \theta_4, \ x_8 = \dot{\theta}_4, \ u_1 = \tau_1, \ u_2 = \tau_2, \ u_3 = \tau_3, \ u_4 = \tau_4 \text{ and } \sum_{j=1}^2 \bar{q}_j^* \theta_{noise_j}.$$

Therefore, the state-space dynamic model of the FLMA with real physical values can be represented as

$$\begin{aligned} [\dot{x}_1 \ \cdots \ \dot{x}_8]^T &= [f_1(\bar{X}) \ \cdots \ f_8(\bar{X})]^T \\ &+ [\bar{g}_{fb_1}(\bar{X}) \ \cdots \ \bar{g}_{fb_4}(\bar{X})][u_{fb_1}(\bar{X}) \ \cdots \ u_{fb_4}(\bar{X})]^T + \sum_{j=1}^2 \bar{q}_j^* \theta_{noise_j} \end{aligned} \quad (97)$$

$$[y_{o1}(\bar{X}) \ \cdots \ y_{o4}(\bar{X})]^T = [\sigma_{o1}(\bar{X}) \ \cdots \ \sigma_{o4}(\bar{X})]^T \quad (98)$$

$$f_1 \equiv x_2 \quad (99)$$

$$f_2 \equiv -D_{c11}x_2 - D_{c12}x_4 - D_{g1} \quad (100)$$

$$f_3 \equiv x_4 \quad (101)$$

$$f_4 \equiv -D_{c21}x_2 - D_{c22}x_4 - D_{c23}x_6 - D_{c24}x_8 - D_{g2} \quad (102)$$

$$f_5 \equiv x_6 \quad (103)$$

$$f_6 \equiv -D_{c31}x_2 - D_{c32}x_4 - D_{c33}x_6 - D_{c34}x_8 - D_{g3} \quad (104)$$

$$f_7 \equiv x_8 \quad (105)$$

$$f_8 \equiv -D_{c41}x_2 - D_{c42}x_4 - D_{c43}x_6 - D_{c44}x_8 - D_{g4} \quad (106)$$

$$\bar{g}_{fb,1} = [0 \ I_{11} \ 0 \ 0 \ 0 \ 0 \ 0 \ 0]^T \quad (107)$$

$$\bar{g}_{fb,2} = [0 \ 0 \ 0 \ I_{22} \ 0 \ I_{23} \ 0 \ I_{24}]^T \quad (108)$$

$$\bar{g}_{fb,3} = [0 \ 0 \ 0 \ I_{23} \ 0 \ I_{33} \ 0 \ I_{34}]^T \quad (109)$$

$$\bar{g}_{fb,4} = [0 \ 0 \ 0 \ I_{24} \ 0 \ I_{34} \ 0 \ I_{44}]^T \quad (110)$$

$$\bar{q}_1^* \theta_{noise_1} = [\sin t \ 0 \ 0 \ 0 \ 0 \ 0 \ 0 \ 0]^T \quad (111)$$

$$\bar{q}_2^* \theta_{noise_2} = [0 \ 0 \ \sin t \ 0 \ 0 \ 0 \ 0 \ 0]^T \quad (112)$$

$$y_{o1} = \theta_1 + \dot{\theta}_1 = x_1 + \dot{x}_1 \equiv \sigma_{o1} \quad (113)$$

$$y_{o2} = \theta_2 + \dot{\theta}_2 = x_3 + \dot{x}_3 \equiv \sigma_{o2} \quad (114)$$

$$y_{o3} = \theta_3 + \dot{\theta}_3 = x_5 + \dot{x}_5 \equiv \sigma_{o3} \quad (115)$$

$$y_{o4} = \theta_4 + \dot{\theta}_4 = x_7 + \dot{x}_7 \equiv \sigma_{o4} \quad (116)$$

Then the nominal system will be

$$\dot{\bar{X}}(t) = \bar{f}(\bar{X}(t)) + \bar{g}_{fb}(\bar{X}(t))\bar{u}_{fb} \quad (117)$$

$$\bar{y}_o(t) = \bar{\sigma}_o(\bar{X}(t)) \quad (118)$$

and it is assumed to have the vector relative frequency $\{d_{o1}, d_{o2}, d_{o3}, d_{o4}\} = \{1, 1, 1, 1\}$ [39]:

<i>The following condition holds:

$$L_{\bar{g}_{fb,j}} L_f^k \sigma_{oi}(\bar{X}) = 0 \quad (119)$$

for all $1 \leq i, j \leq 4, k < d_{oi} - 1$, where the symbol L is the Lie operator.

<ii>The square matrix

$$A \equiv \begin{bmatrix} L_{g_{fb_1}} L_f^{d_{o1}-1} \sigma_{o1}(\bar{X}) & \cdots & L_{g_{fb_m}} L_f^{d_{o1}-1} \sigma_{o1}(\bar{X}) \\ \vdots & & \vdots \\ L_{g_{fb_1}} L_f^{d_{om}-1} \sigma_{om}(\bar{X}) & \cdots & L_{g_{fb_m}} L_f^{d_{om}-1} \sigma_{om}(\bar{X}) \end{bmatrix} \quad (120)$$

has nonsingular property. The norms of pre-specified tracking signals $y_{track}^i, 1 \leq i \leq 4$ and its first d_{oi} derivatives are bounded by positive constants B_{track}^i as

$$\left\| \left[y_{track}^i, y_{track}^{i(1)}, \dots, y_{track}^{i(d_{oi})} \right] \right\| \leq B_{track}^i, 1 \leq i \leq 4 \quad (121)$$

and the spanning distribution

$$G \equiv span\{\bar{g}_{fb_1}, \bar{g}_{fb_2}, \bar{g}_{fb_3}, \bar{g}_{fb_4}\} \quad (122)$$

is involutive.

3. Robust and Tracking Controller Design of the FLMA System

Since the FLMA system has the well-defined relative degree property and involutive distribution performance, then the mapping

$$\varphi: \mathfrak{R}^n \rightarrow \mathfrak{R}^n \quad (123)$$

defined as

$$\begin{aligned} \bar{\xi}_{lin_i} &\equiv \left[\xi_{lin_{-1}}^i \quad \cdots \quad \xi_{lin_{-d_{oi}}}^i \right]^T \equiv \left[\phi_{lin_{-1}}^i \quad \cdots \quad \phi_{lin_{-d_{oi}}}^i \right]^T \\ &\equiv \left[L_f^0 \sigma_{oi} \quad \cdots \quad L_f^{d_{oi}-1} \sigma_{oi} \right]^T, 1 \leq i \leq 4 \end{aligned} \quad (124)$$

$$d_o \equiv d_{o1} + d_{o2} + d_{o3} + d_{o4} = 4 \quad (125)$$

$$\varphi_{non_k} \equiv \eta_{non_k}, k = d_o + 1, d_o + 2, \dots, n \quad (126)$$

and

$$L_{g_{fb_j}} \varphi_{non_k} = 0, k = d_o + 1, d_o + 2, \dots, n, 1 \leq j \leq 4 \quad (127)$$

$$\bar{\xi}_{lin} \equiv \left[\xi_{lin_{-1}} \quad \xi_{lin_{-2}} \quad \cdots \quad \xi_{lin_{-d_o}} \right]^T \quad (128)$$

$$\bar{\eta}_{non} \equiv \left[\eta_{non_{-d_o+1}} \quad \eta_{non_{-d_o+2}} \quad \cdots \quad \eta_{non_{-n}} \right]^T \quad (129)$$

$$\begin{aligned} \bar{\rho}_{non} &\equiv \left[L_f \varphi_{non_{-d_o+1}} \quad L_f \varphi_{non_{-d_o+2}} \quad \cdots \quad L_f \varphi_{non_{-n}} \right]^T \\ &\equiv \left[\rho_{non_{-d_o+1}} \quad \rho_{non_{-d_o+2}} \quad \cdots \quad \rho_{non_{-n}} \right]^T \end{aligned} \quad (130)$$

is an one-to-one and onto, infinitely continuous and differentiable function according to reference [39,40], i.e,

$$\bar{\xi}_{lin_{-1}} \equiv \xi_{lin_{-1}}^1 = \phi_{lin_{-1}}^1 \equiv L_f^0 \sigma_{o1} = x_1 + x_2, \quad (131)$$

$$\bar{\xi}_{lin_{-2}} \equiv \xi_{lin_{-1}}^2 = \phi_{lin_{-1}}^2 \equiv L_f^0 \sigma_{o2} = x_3 + x_4, \quad (132)$$

$$\bar{\xi}_{lin_{-3}} \equiv \xi_{lin_{-1}}^3 = \phi_{lin_{-1}}^3 \equiv L_f^0 \sigma_{o3} = x_5 + x_6, \quad (133)$$

$$\bar{\xi}_{lin_{-4}} \equiv \xi_{lin_{-1}}^4 = \phi_{lin_{-1}}^4 \equiv L_f^0 \sigma_{o4} = x_7 + x_8, \quad (134)$$

$$\eta_{non_5} \equiv \phi_{non_5} \equiv x_1 - y_{track}^1 \quad (135)$$

$$\eta_{non_6} \equiv \phi_{non_6} \equiv x_3 - y_{track}^2 \quad (136)$$

$$\eta_{non_7} \equiv \phi_{non_7} \equiv x_5 - y_{track}^3 \quad (137)$$

$$\eta_{non_8} \equiv \phi_{non_8} \equiv x_7 - y_{track}^4 \quad (138)$$

Assume that the nonlinear FLMA system possesses the well-defined involutive property. Then the mapping φ defined by (124)~(127) is a one-to-one and onto, infinitely continuous and differentiable function and it will transform original nonlinear system into partially linear subsystem and partially nonlinear subsystem as follows [39,40] as follows:

$$\begin{aligned} \dot{\xi}_{lin_1}^1 &= \frac{\partial \sigma_{o1}}{\partial \bar{X}} \left[\bar{f} + g_{fb} \cdot \bar{u}_{fb} + \sum_{j=1}^p \bar{q}_j^* (\theta_{un_j} + \theta_{noise_j}) \right] \\ &= \xi_{lin_2}^1 + \sum_{j=1}^p \left(\frac{\partial \sigma_{o1}}{\partial \bar{X}} \bar{q}_j^* \right) (\theta_{un_j} + \theta_{noise_j}) \end{aligned} \quad (139)$$

⋮

$$\begin{aligned} \dot{\xi}_{lin_d_{o1}-1}^1 &= \frac{\partial L_f^{d_{o1}-2} \sigma_{o1}}{\partial \bar{X}} \left[\bar{f} + g_{fb} \cdot \bar{u}_{fb} + \sum_{j=1}^p \bar{q}_j^* (\theta_{un_j} + \theta_{noise_j}) \right] \\ &= \xi_{lin_d_{o1}}^1 + \sum_{j=1}^p \left(\frac{\partial L_f^{d_{o1}-2} \sigma_{o1}}{\partial \bar{X}} \bar{q}_j^* \right) (\theta_{un_j} + \theta_{noise_j}) \end{aligned} \quad (140)$$

$$\begin{aligned} \dot{\xi}_{lin_d_{o1}}^1 &= \frac{\partial \varphi_{lin_d_{o1}}^1}{\partial \bar{X}} \frac{d\bar{X}}{dt} \\ &= \frac{\partial L_f^{d_{o1}-1} \sigma_{o1}}{\partial \bar{X}} \left[\bar{f} + g_{fb} \cdot \bar{u}_{fb} + \sum_{j=1}^p \bar{q}_j^* (\theta_{un_j} + \theta_{noise_j}) \right] \\ &= L_{\bar{f}}^{d_{o1}} \sigma_{o1} + L_{g_{fb,1}} L_{\bar{f}}^{d_{o1}-1} \sigma_{o1} u_1 + \dots + L_{g_{fb,m}} L_{\bar{f}}^{d_{o1}-1} \sigma_{o1} u_m \\ &\quad + \sum_{j=1}^p \left(\frac{\partial L_f^{d_{o1}-1} \sigma_{o1}}{\partial \bar{X}} \bar{q}_j^* \right) (\theta_{un_j} + \theta_{noise_j}) \end{aligned} \quad (141)$$

⋮

$$\begin{aligned} \dot{\xi}_{lin_1}^4 &= \frac{\partial \sigma_{o4}}{\partial \bar{X}} \left[\bar{f} + g_{fb} \cdot \bar{u}_{fb} + \sum_{j=1}^p \bar{q}_j^* (\theta_{un_j} + \theta_{noise_j}) \right] \\ &= \xi_{lin_2}^4 + \sum_{j=1}^p \left(\frac{\partial \sigma_{o4}}{\partial \bar{X}} \bar{q}_j^* \right) (\theta_{un_j} + \theta_{noise_j}) \end{aligned} \quad (142)$$

⋮

$$\begin{aligned} \dot{\xi}_{lin_d_{o4}-1}^4 &= \frac{\partial L_f^{d_{o4}-2} \sigma_{o4}}{\partial \bar{X}} \left[\bar{f} + g_{fb} \cdot \bar{u}_{fb} + \sum_{j=1}^p \bar{q}_j^* (\theta_{un_j} + \theta_{noise_j}) \right] \\ &= \xi_{lin_d_{o4}}^4 + \sum_{j=1}^p \left(\frac{\partial L_f^{d_{o4}-2} \sigma_{o4}}{\partial \bar{X}} \bar{q}_j^* \right) (\theta_{un_j} + \theta_{noise_j}) \end{aligned} \quad (143)$$

$$\begin{aligned}
& \dot{\xi}_{lin_d_{o4}}^4 \\
&= \frac{\partial L_f^{d_{o4}-1} \sigma_{o4}}{\partial \bar{X}} \left[\bar{f} + \underline{g}_{fb} \cdot \bar{u}_{fb} + \sum_{j=1}^p \bar{q}_j^* (\theta_{un_j} + \theta_{noise_j}) \right] \\
&= L_{\bar{f}}^{d_{o4}} \sigma_{o4} + L_{\bar{g}_{fb_1}} L_{\bar{f}}^{d_{o4}-1} \sigma_{o4} u_{fb_1} + \dots \\
&+ L_{\bar{g}_{fb_4}} L_{\bar{f}}^{d_{o4}-1} \sigma_{o4} u_{fb_4} \\
&+ \sum_{j=1}^p \left(\frac{\partial L_f^{d_{o4}-1} \sigma_{o4}}{\partial \bar{X}} \bar{q}_j^* \right) (\theta_{un_j} + \theta_{noise_j})
\end{aligned} \tag{144}$$

$$\begin{aligned}
\dot{\eta}_{non_k} &= \frac{\partial \varphi_{non_k}}{\partial \bar{X}} \left[\bar{f} + \underline{g}_{fb} \cdot \bar{u}_{fb} + \sum_{j=1}^p \bar{q}_j^* (\theta_{un_j} + \theta_{noise_j}) \right] \\
&= \bar{\rho}_{non_k} + \sum_{j=1}^p \left(\frac{\partial \varphi_{non_k}}{\partial \bar{X}} \bar{q}_j^* \right) (\theta_{un_j} + \theta_{noise_j})
\end{aligned} \tag{145}$$

Since

$$u_{ci} \equiv L_{\bar{f}}^{d_{oi}} \sigma_{oi} \tag{146}$$

$$u_{dij} \equiv L_{\bar{g}_{fb_j}} L_{\bar{f}}^{d_{oi}-1} \sigma_{oi}, \tag{147}$$

the transformed dynamics of nonlinear FLMA system (139)~(145) can be rewritten to be

$$\begin{aligned}
\dot{\xi}_{lin_1}^1(t) &= \dot{\xi}_{lin_d_{o1}}^1 = u_{c1} + u_{d11} u_{fb_1} + \dots + u_{d14} u_{fb_4} \\
&+ \sum_{j=1}^p \left(\frac{\partial}{\partial \bar{X}} L_{\bar{f}}^{d_{o1}-1} \sigma_{o1} \right) \bar{q}_j^* (\theta_{un_j} + \theta_{noise_j})
\end{aligned} \tag{148}$$

⋮

$$\begin{aligned}
\dot{\xi}_{lin_1}^4 &= \dot{\xi}_{lin_d_{o4}}^4 = u_{c4} + u_{d41} u_{fb_1} + \dots + u_{d44} u_{fb_4} \\
&+ \sum_{j=1}^p \left(\frac{\partial}{\partial \bar{X}} L_{\bar{f}}^{d_{o4}-1} \sigma_{o4} \right) \bar{q}_j^* (\theta_{un_j} + \theta_{noise_j})
\end{aligned} \tag{149}$$

$$\begin{aligned}
\dot{\eta}_{non_k} &= \bar{\rho}_{non_k} \\
&+ \sum_{j=1}^p \left(\frac{\partial}{\partial \bar{X}} \varphi_{non_k}(\bar{X}) \right) \bar{q}_j^* (\theta_{un_j} + \theta_{noise_j}), k = d_o + 1, \dots, n
\end{aligned} \tag{150}$$

$$y_{oi} = \xi_{lin_1}^i, 1 \leq i \leq 4 \tag{151}$$

Hence

$$\begin{aligned}
\begin{bmatrix} \dot{\xi}_{l_{-d_{o1}}}^1 \\ \dot{\xi}_{l_{-d_{o2}}}^2 \\ \dot{\xi}_{l_{-d_{o3}}}^3 \\ \dot{\xi}_{l_{-d_{o4}}}^4 \end{bmatrix} &= \begin{bmatrix} \xi_{l_{-1}}^1 \\ \xi_{l_{-1}}^2 \\ \xi_{l_{-1}}^3 \\ \xi_{l_{-1}}^4 \end{bmatrix} = \begin{bmatrix} u_{c1} \\ u_{c2} \\ u_{c3} \\ u_{c4} \end{bmatrix} + \begin{bmatrix} u_{d11} & u_{d12} & u_{d13} & u_{d14} \\ u_{d21} & u_{d22} & u_{d23} & u_{d24} \\ u_{d31} & u_{d32} & u_{d33} & u_{d34} \\ u_{d41} & u_{d42} & u_{d43} & u_{d44} \end{bmatrix} \begin{bmatrix} u_{fb_{-1}} \\ u_{fb_{-2}} \\ u_{fb_{-3}} \\ u_{fb_{-4}} \end{bmatrix} \\
&+ \begin{bmatrix} \sum_{j=1}^p \left(\frac{\partial}{\partial X} L_f^{d_{o1}-1} \sigma_{o1} \right) \bar{q}_j^* (\theta_{un_j} + \theta_{noise_{-j}}) \\ \sum_{j=1}^p \left(\frac{\partial}{\partial X} L_f^{d_{o2}-1} \sigma_{o2} \right) \bar{q}_j^* (\theta_{un_j} + \theta_{noise_{-j}}) \\ \sum_{j=1}^p \left(\frac{\partial}{\partial X} L_f^{d_{o3}-1} \sigma_{o3} \right) \bar{q}_j^* (\theta_{un_j} + \theta_{noise_{-j}}) \\ \sum_{j=1}^p \left(\frac{\partial}{\partial X} L_f^{d_{o4}-1} \sigma_{o4} \right) \bar{q}_j^* (\theta_{un_j} + \theta_{noise_{-j}}) \end{bmatrix} \quad (152)
\end{aligned}$$

$$\begin{aligned}
\begin{bmatrix} \dot{\eta}_{non_{-d_o+1}} & \dots & \dot{\eta}_{non_{-n}}(t) \end{bmatrix}^T &= \begin{bmatrix} \rho_{non_{-d_o+1}} & \dots & \rho_{non_{-n}} \end{bmatrix}^T \\
&+ \begin{bmatrix} \sum_{j=1}^p \left(\frac{\partial}{\partial X} \varphi_{non_{-d_o+1}} \right) \bar{q}_j^* (\theta_{un_j} + \theta_{noise_{-j}}) & \dots & \\ \sum_{j=1}^p \left(\frac{\partial}{\partial X} \varphi_{non_{-n}} \right) \bar{q}_j^* (\theta_{un_j} + \theta_{noise_{-j}}) \end{bmatrix}^T \quad (153)
\end{aligned}$$

$$y_{oi} = \xi_{lin_{-1}}^i \quad (154)$$

To build the robust feedback linearization controller

$$\bar{u}_{fb} = A^{-1} \{-\bar{u}_b + \bar{u}_v\} \quad (155)$$

we use the vector

$$\begin{aligned}
\bar{u}_b &\equiv [u_{b1} \quad u_{b2} \quad u_{b3} \quad u_{b4}]^T \equiv [L_f^{d_{o1}} \sigma_{o1} \quad L_f^{d_{o2}} \sigma_{o2} \quad L_f^{d_{o3}} \sigma_{o3} \quad L_f^{d_{o4}} \sigma_{o4}]^T \\
&= [u_{c1} \quad u_{c2} \quad u_{c3} \quad u_{c4}]^T \equiv \bar{u}_c \quad (156)
\end{aligned}$$

and the virtual input [39]

$$\bar{u}_v \equiv [u_{v1} \quad u_{v2} \quad u_{v3} \quad u_{v4}]^T \quad (157)$$

Then we can transform (152) into the following model

$$\begin{aligned}
\begin{bmatrix} \dot{\xi}_{l_{-d_{o1}}}^1 \\ \dot{\xi}_{l_{-d_{o2}}}^2 \\ \dot{\xi}_{l_{-d_{o3}}}^3 \\ \dot{\xi}_{l_{-d_{o4}}}^4 \end{bmatrix} &= \begin{bmatrix} \dot{\xi}_{l_{-1}}^1 \\ \dot{\xi}_{l_{-1}}^2 \\ \dot{\xi}_{l_{-1}}^3 \\ \dot{\xi}_{l_{-1}}^4 \end{bmatrix} \\
&= \begin{bmatrix} u_{v1} \\ u_{v2} \\ u_{v3} \\ u_{v4} \end{bmatrix} + \begin{bmatrix} \sum_{j=1}^p \left(\frac{\partial}{\partial \bar{X}} L_f^{d_{o1}-1} \sigma_{o1} \right) \bar{q}_j^* (\theta_{un,j} + \theta_{noise,j}) \\ \sum_{j=1}^p \left(\frac{\partial}{\partial \bar{X}} L_f^{d_{o2}-1} \sigma_{o2} \right) \bar{q}_j^* (\theta_{un,j} + \theta_{noise,j}) \\ \sum_{j=1}^p \left(\frac{\partial}{\partial \bar{X}} L_f^{d_{o3}-1} \sigma_{o3} \right) \bar{q}_j^* (\theta_{un,j} + \theta_{noise,j}) \\ \sum_{j=1}^p \left(\frac{\partial}{\partial \bar{X}} L_f^{d_{o4}-1} \sigma_{o4} \right) \bar{q}_j^* (\theta_{un,j} + \theta_{noise,j}) \end{bmatrix} \quad (158)
\end{aligned}$$

From (158), we get

$$\begin{aligned}
\dot{\xi}_{l_{-1}}^i(t) &= \dot{\xi}_{l_{-d_{oi}}}^i = [1] u_{vi} + \left[\sum_{j=1}^p \left(\frac{\partial}{\partial \bar{X}} L_f^{d_{oi}-1} \sigma_{oi} \right) \bar{q}_j^* (\theta_{un,j} + \theta_{noise,j}) \right] \\
d_{oi} &= 1, i = 1, 2, 3, 4 \quad (159)
\end{aligned}$$

Next we will demonstrate in detail how to design the robust and tracking controller $\bar{u}_{fb} = A^{-1} \{-\bar{u}_b + \bar{u}_v\}$ with the pre-specified tracking signals $y_{track}^1 = y_{track}^2 = y_{track}^3 = y_{track}^4 = \pi/6$.

The initial values of the states are set to be

$$\bar{x}(0) \equiv [1 \ 0 \ 1 \ 0 \ 1 \ 0 \ 1 \ 0]^T \quad (160)$$

The desired robust and tracking controller is built by

$$\begin{aligned}
u_{vi} &\equiv y_{track}^i \quad (d_{oi}) - \varepsilon^{-d_{oi}} \alpha_i^j \left[L_f^0 \sigma_{oi}(\bar{X}) - y_{track}^i \right] \\
&- \varepsilon^{1-d_{oi}} \alpha_i^j \left[L_f^1 \sigma_{oi}(\bar{X}) - y_{track}^i \quad (1) \right] - \dots \\
&- \varepsilon^{-1} \alpha_i^j \left[L_f^{d_{oi}-1} \sigma_{oi}(\bar{X}) - y_{track}^i \quad (d_{oi}-1) \right], 1 \leq i \leq 4 \quad (161)
\end{aligned}$$

where y_{track}^i is the desired tracking signal and $\alpha_{d_{oi}}^i$ are elements of the Hurwitz matrix shown by

$$A_c^i \equiv \begin{bmatrix} 0 & 1 & 0 & \dots & 0 \\ 0 & 0 & 1 & \dots & 0 \\ \vdots & & & & \vdots \\ 0 & 0 & 0 & \dots & 1 \\ -\alpha_1^i & -\alpha_2^i & -\alpha_3^i & \dots & -\alpha_{d_{oi}}^i \end{bmatrix}_{d_{oi} \times d_{oi}} = [-50]_{1 \times 1}, i = 1, \dots, 4 \quad (162)$$

Based on feedback linearization approach, then we propose the robust controller with the pre-specified tracking signals $y_{track}^1 = y_{track}^2 = y_{track}^3 = y_{track}^4 = \pi/6$ as follows:

$$\bar{u}_{fb} = A^{-1} (-\bar{u}_b + \bar{u}_v) = A^{-1} \left(-[u_{b1} \ \dots \ u_{b4}]^T + [u_{v1} \ \dots \ u_{v4}]^T \right) \quad (163)$$

$$A^{-1} = \begin{bmatrix} D_{11} & 0 & 0 & 0 \\ 0 & D_{22} & D_{23} & D_{24} \\ 0 & D_{23} & D_{33} & D_{34} \\ 0 & D_{24} & D_{34} & D_{44} \end{bmatrix} \quad (164)$$

$$\bar{u}_v = \begin{bmatrix} -\mathcal{E}^{-1}(50)(x_1 + x_2 - \pi/6) \\ -\mathcal{E}^{-1}(50)(x_3 + x_4 - \pi/6) \\ -\mathcal{E}^{-1}(50)(x_5 + x_6 - \pi/6) \\ -\mathcal{E}^{-1}(50)(x_7 + x_8 - \pi/6) \end{bmatrix} \quad (165)$$

$$\bar{u}_b = \begin{bmatrix} f_1 + f_2 \\ f_3 + f_4 \\ f_5 + f_6 \\ f_7 + f_8 \end{bmatrix} \quad (166)$$

$$u_1 = D_{11} [-f_1 - f_2 - \mathcal{E}^{-1}(50)(x_1 + x_2 - \pi/6)] \quad (167)$$

$$\begin{aligned} u_2 &= D_{22} [-f_3 - f_4 - \mathcal{E}^{-1}(50)(x_3 + x_4 - \pi/6)] \\ &+ D_{23} [-f_5 - f_6 - \mathcal{E}^{-1}(50)(x_5 + x_6 - \pi/6)] \\ &+ D_{24} [-f_7 - f_8 - \mathcal{E}^{-1}(50)(x_7 + x_8 - \pi/6)] \end{aligned} \quad (168)$$

$$\begin{aligned} u_3 &= D_{23} [-f_3 - f_4 - \mathcal{E}^{-1}(50)(x_3 + x_4 - \pi/6)] \\ &+ D_{33} [-f_5 - f_6 - \mathcal{E}^{-1}(50)(x_5 + x_6 - \pi/6)] \\ &+ D_{34} [-f_7 - f_8 - \mathcal{E}^{-1}(50)(x_7 + x_8 - \pi/6)] \end{aligned} \quad (169)$$

$$\begin{aligned} u_4 &= D_{24} [-f_3 - f_4 - \mathcal{E}^{-1}(50)(x_3 + x_4 - \pi/6)] \\ &+ D_{34} [-f_5 - f_6 - \mathcal{E}^{-1}(50)(x_5 + x_6 - \pi/6)] \\ &+ D_{44} [-f_7 - f_8 - \mathcal{E}^{-1}(50)(x_7 + x_8 - \pi/6)] \end{aligned} \quad (170)$$

For the convenience of the following discussions, let's define some related parameters as

$$e_j^i \equiv \xi_{lin_j}^i - y_{track}^{i(j-1)} \quad (171)$$

$$e_{track}^i \equiv [e_1^i \ e_2^i \ \dots \ e_{d_{oi}}^i]^T \in \mathfrak{R}^{d_{oi}} \quad (172)$$

$$\bar{e}_j^i \equiv \mathcal{E}^{j-1} e_j^i, i=1,2,\dots,4, j=1,2,\dots,d_{oi} \quad (173)$$

$$\bar{e}_{track}^i \equiv [\bar{e}_1^i \ \bar{e}_2^i \ \dots \ \bar{e}_{d_{oi}}^i(t)]^T \in \mathfrak{R}^{d_{oi}} \quad (174)$$

$$\bar{e}_{track} \equiv [\bar{e}_{track}^1 \ \bar{e}_{track}^2 \ \dots \ \bar{e}_{track}^4]^T \in \mathfrak{R}^{d_o} \quad (175)$$

$$\bar{B}^i \equiv [0 \ 0 \ \dots \ 0 \ 1]_{d_{oi} \times 1}^T, 1 \leq i \leq 4 \quad (176)$$

$$\begin{aligned} &\bar{\rho}_{non}(\bar{\xi}_{lin}, \bar{\eta}_{non}) \\ &= [L_f \varphi_{non_d_o+1} \ L_f \varphi_{non_d_o+2} \ \dots \ L_f \varphi_{non_n}]^T \\ &= [\rho_{non_d_o+1} \ \rho_{non_d_o+2} \ \dots \ \rho_{non_n}]^T \end{aligned} \quad (177)$$

where the Lyapunov system matrix A_c^i is a Hurwitz matrix whose eigenvalues lies in the left half coordinate plane and one can use Matlab to obtain the adjoining Lyapunov system matrix $P_{Lyap}^i > 0$ of the following Lyapunov equation:

$$(A_c^i)^T P_{Lyap}^i + P_{Lyap}^i A_c^i = -I \quad (178)$$

$$\gamma_{\max}(P_{Lyap}^i) \equiv \max. \text{ eigenvalue of } P_{Lyap}^i \quad (179)$$

$$\gamma_{\min}(P_{Lyap}^i) \equiv \min. \text{ eigenvalue of } P_{Lyap}^i \quad (180)$$

$$\begin{aligned} \gamma_{\max}^* &\equiv \max\{\gamma_{\max}(P_{Lyap}^1), \gamma_{\max}(P_{Lyap}^2), \dots, \gamma_{\max}(P_{Lyap}^4)\} \\ &\equiv \max\{0.01, 0.01, \dots, 0.01\} = 0.01 \end{aligned} \quad (181)$$

$$\begin{aligned} \gamma_{\min}^* &\equiv \min\{\gamma_{\min}(P_{Lyap}^1), \gamma_{\min}(P_{Lyap}^2), \dots, \gamma_{\min}(P_{Lyap}^4)\} \\ &\equiv \min\{0.01, 0.01, \dots, 0.01\} = 0.01 \end{aligned} \quad (182)$$

and

$$P_{Lyap}^1 = P_{Lyap}^2 = P_{Lyap}^3 = P_{Lyap}^4 = 0.01 \quad (183)$$

To demonstrate further the complete feedback linearization control design of nonlinear FLMA system, let's define one assumption and two definitions as

Assumption 1. The following inequality holds:

$$\|\bar{\rho}_{non_t}(t, \bar{\eta}_{non}, \bar{e}_{track}) - \bar{\rho}_{non_t}(t, \bar{\eta}_{non}, 0)\| \leq M_{non} (\|\bar{e}_{track}\|) \quad (184)$$

where $M_{non} > 0$ and $\bar{\rho}_{non_t}(t, \bar{\eta}_{non}, \bar{e}_{track}) \equiv \bar{\rho}_{non}(\bar{\xi}_{lin}, \bar{\eta}_{non})$.

Definition 1.

Consider a nonlinear system $\dot{\bar{X}} = \bar{f}(t, \bar{X}, \bar{u}_{input})$ with an Lipschitz input \bar{u}_{input} , where \bar{X} is Lipschitz state variable, $\bar{f}: [0, \infty) \times \mathfrak{R}^n \times \mathfrak{R}^n \rightarrow \mathfrak{R}^n$ is differentiable and infinitely continuous. This system is defined to be input-to-state stable if

$$\|\bar{X}(t)\| \leq \gamma(\|\bar{X}(t_0)\|, t - t_0) + \kappa \left(\sup_{t_0 \leq \tau \leq t} \|\bar{u}_{input}(\tau)\| \right) \quad (185)$$

where κ is a K -class function and γ denotes a KL -class function.

Definition 2.

A nonlinear system with noise input \bar{u}_{noise} is defined to possess the almost disturbance decoupling performance, if the following properties hold:

<i>The nonlinear system has input-to-state stable property for noise input \bar{u}_{noise} .

<ii>Output tracking errors meet the following two inequalities for initial time t_0 and the initial state $\bar{X}(t_0)$:

$$|y_{oi}(t) - y_{track}^i(t)| \leq \kappa_1 (\|\bar{X}(t_0)\|, t - t_0) + \frac{1}{\sqrt{\kappa_2}} \kappa_3 \left(\sup_{t_0 \leq \tau \leq t} \|\bar{u}_{noise}(\tau)\| \right) \quad (186)$$

and

$$\int_{t_0}^t [y_{oi}(\tau) - y_{track}^i(\tau)]^2 d\tau \leq \left[\kappa_5 (\|\bar{X}_{e0}\|) + \int_{t_0}^t \kappa_3 (\|\bar{u}_{noise}(\tau)\|^2) d\tau \right] \quad (187)$$

where κ_1 belongs to KL -class function, κ_2 and κ_4 are positive constants, and κ_3, κ_5 belong to K -class functions. From (159), we get

$$\begin{aligned} \left[\dot{\zeta}_{lin_1}^i(t) - \dot{y}_{track}^i \right] &= \left[\dot{\zeta}_{lin_d_{oi}}^i - \dot{y}_{track}^{i(d_{oi}-1)} \right] = [1] \left(u_{vi} - y_{track}^{i(d_{oi})} \right) \\ &+ \left[\sum_{j=1}^p \left(\frac{\partial}{\partial \bar{X}} L_f^{d_{oi}-1} \sigma_{oi} \right) \bar{q}_j^* (\theta_{un_j} + \theta_{noise_j}) \right] \\ d_{oi} &= 1, i = 1, 2, 3, 4 \end{aligned} \quad (188)$$

From (171), (173) and (188), we obtain

$$\left[\varepsilon^{1-d_{oi}} \bar{e}_{d_{oi}}^i \right] = [1] \left(u_{vi} - y_{track}^{i(d_{oi})} \right) + \left[\sum_{j=1}^p \left(\frac{\partial}{\partial \bar{X}} L_f^{d_{oi}-1} \sigma_{oi} \right) \bar{q}_j^* (\theta_{un_j} + \theta_{noise_j}) \right] \quad (189)$$

Substituting (161) and (162) into (189) obtains

$$\begin{aligned} \varepsilon \left[\bar{e}_{d_{oi}}^i \right] &= [-\alpha_{d_{oi}}^i] \left(\bar{e}_{d_{oi}}^i \right) + \left[\varepsilon \sum_{j=1}^p \left(\frac{\partial}{\partial \bar{X}} L_f^{d_{oi}-1} \sigma_{oi} \right) \bar{q}_j^* (\theta_{un_j} + \theta_{noise_j}) \right] \\ i &= 1, \dots, 4 \end{aligned} \quad (190)$$

Then, from (145), (153), (162), (174) and (190), we obtain

$$\varepsilon \bar{e}_{track}^i = A_c^i \bar{e}_{track}^i + \varphi_{\zeta_{lin}}^i (\bar{\theta}_{noise} + \bar{\theta}_{un}), i = 1, \dots, 4 \quad (191)$$

$$\begin{aligned} \dot{\bar{\eta}}_{non} &= \bar{\rho}_{non} (\bar{\zeta}_{lin}, \bar{\eta}_{non}) + \varphi_{\bar{\eta}_{non}} (\bar{\theta}_{noise} + \bar{\theta}_{un}) \\ &\equiv \bar{\rho}_{non_i}(t, \bar{\eta}_{non}, \bar{e}_{track}) + \varphi_{\bar{\eta}_{non}} (\bar{\theta}_{noise} + \bar{\theta}_{un}) \end{aligned} \quad (192)$$

$$y_{oi} = \zeta_{lin_1}^i, i = 1, \dots, 4 \quad (193)$$

where

$$\begin{aligned} \varphi_{\zeta_{lin}}^i(\varepsilon) &\equiv \begin{bmatrix} \varepsilon \left(\frac{\partial}{\partial \bar{X}} \sigma_{oi} \right) \bar{q}_1^* & \dots & \varepsilon \left(\frac{\partial}{\partial \bar{X}} \sigma_{oi} \right) \bar{q}_p^* \\ \vdots & & \vdots \\ \varepsilon^{d_{oi}} \left(\frac{\partial}{\partial \bar{X}} L_f^{d_{oi}-1} \sigma_{oi} \right) \bar{q}_1^* & \dots & \varepsilon^{d_{oi}} \left(\frac{\partial}{\partial \bar{X}} L_f^{d_{oi}-1} \sigma_{oi} \right) \bar{q}_p^* \end{bmatrix} \\ i &= 1, \dots, 4 \end{aligned} \quad (194)$$

$$\varphi_{\eta_{non}}(\varepsilon) \equiv \begin{bmatrix} \left(\frac{\partial}{\partial \bar{X}} \varphi_{non_d_o+1} \right) \bar{q}_1^* & \dots & \left(\frac{\partial}{\partial \bar{X}} \varphi_{non_d_o+1} \right) \bar{q}_p^* \\ \vdots & & \vdots \\ \left(\frac{\partial}{\partial \bar{X}} \varphi_{non_n} \right) \bar{q}_1^* & \dots & \left(\frac{\partial}{\partial \bar{X}} \varphi_{non_n} \right) \bar{q}_p^* \end{bmatrix} \quad (195)$$

$$\bar{\theta}_{noise} \equiv [\theta_{noise_1}(t) \ \cdots \ \theta_{noise_p}(t)]^T \quad (196)$$

$$\bar{\theta}_{un} \equiv [\theta_{un_1}(t) \ \cdots \ \theta_{un_p}(t)]^T \quad (197)$$

It is worth noting that the one-to-one and onto, infinitely continuous and differentiable function converts the original nonlinear FLMA into a partially nonlinear subsystem and partially linear subsystem whose state variables are denoted by $\xi_{lin_1}^1, \xi_{lin_1}^2, \xi_{lin_1}^3, \xi_{lin_1}^4$ and $\eta_{non_5} \sim \eta_{non_8}$, respectively. In order to meet the requirements (184) and

$$\omega_{non1} \|\bar{\eta}_{non}\|^2 \leq J_{non}(\bar{\eta}_{non}) \leq \omega_{non2} \|\bar{\eta}_{non}\|^2 \quad (198)$$

$$\nabla_t J_{non} + (\nabla_{\bar{\eta}_{non}} J_{non})^T \bar{\rho}_{non}(t, \bar{\eta}_{non}, 0) \leq -16\alpha_x J_{non} \quad (199)$$

$$\|\nabla_{\bar{\eta}_{non}} J_{non}\| \leq \omega_{non3} \|\bar{\eta}_{non}\|, \omega_{non3} > 0 \quad (200)$$

we construct J_{non} and W_{lin} to be the Lyapunov functions of nonlinear subsystem (192) and linear subsystem (191), respectively and then combine these Lyapunov functions to be a composite Lyapunov function $J_{lin+non}$ as follows:

$$\begin{aligned} J_{lin+non} &\equiv J_{non} + k(\varepsilon)W_{lin} \equiv J_{non} \\ &+ k(\varepsilon) \left(W_{lin}^1(\overline{e_{track}^1}) + W_{lin}^2(\overline{e_{track}^2}) + W_{lin}^3(\overline{e_{track}^3}) + W_{lin}^4(\overline{e_{track}^4}) \right) \end{aligned} \quad (201)$$

where the function $k(\varepsilon): \mathfrak{R}^+ \rightarrow \mathfrak{R}^+$ satisfies $\lim_{\varepsilon \rightarrow 0} k(\varepsilon) = 0$ and

$$\lim_{\varepsilon \rightarrow 0} \frac{\varepsilon}{k(\varepsilon)} = 0 \quad (202)$$

$$k(\varepsilon) = 20000\sqrt{\varepsilon} \quad (203)$$

$$W_{lin}^i \equiv \frac{1}{2} \overline{e_{track}^i}^T P_{Lyap}^i \overline{e_{track}^i} = 0.005 \overline{e_{track}^i}^T \overline{e_{track}^i}, i = 1, \dots, 4 \quad (204)$$

$$J_{non} \equiv \eta_{non_5}^2 + \dots + \eta_{non_8}^2, \quad (205)$$

$$\omega_{non1} \|\bar{\eta}_{non}\|^2 \leq V_{non} \leq \omega_{non2} \|\bar{\eta}_{non}\|^2, \omega_{non1} = 1, \omega_{non2} = 1 \quad (206)$$

$$\bar{\rho}_{non_t}(t, \bar{\eta}_{non}, \overline{e_{track}}) = [\overline{e_1^1} - \eta_{non_5} \ \overline{e_1^2} - \eta_{non_6} \ \overline{e_1^3} - \eta_{non_7} \ \overline{e_1^4} - \eta_{non_8}]^T \quad (207)$$

$$\begin{aligned} &\|\bar{\rho}_{non_t}(t, \bar{\eta}_{non}, \overline{e_{track}}) - \bar{\rho}_{non_t}(t, \bar{\eta}_{non}, 0)\|^2 \\ &= \left[(\overline{e_1^1})^2 + (\overline{e_1^2})^2 + (\overline{e_1^3})^2 + (\overline{e_1^4})^2 \right] \leq M_{non} (\|\overline{e_{track}}\|), M_{non} = 1 \end{aligned} \quad (208)$$

$$\begin{aligned} \|\nabla_{\bar{\eta}_{non}} J_{non}\| &= \left\| [2\eta_{non_5} \ 2\eta_{non_6} \ 2\eta_{non_7} \ 2\eta_{non_8}] \right\| \\ &= 2\sqrt{\eta_{non_5}^2 + \eta_{non_6}^2 + \eta_{non_7}^2 + \eta_{non_8}^2} \leq \omega_{non3} \|\bar{\eta}_{non}\|, \omega_{non3} = 2 \end{aligned} \quad (209)$$

$$\begin{aligned} & \nabla_t J_{non} + (\nabla_{\bar{\eta}_{non}} J_{non})^T \bar{\rho}_{non_t}(t, \bar{\eta}_{non}, 0) \\ & = -2(\eta_{non_5}^2 + \eta_{non_6}^2 + \eta_{non_7}^2 + \eta_{non_8}^2) \leq -16\alpha_x(\bar{\eta}_{non}), \alpha_x = 0.125 \end{aligned} \quad (210)$$

Then, the differentiation of the composite Lyapunov function $J_{lin+non}$ is described as

$$\begin{aligned} & \dot{J}_{lin+non} \\ & = \left[\nabla_t J_{non} + (\nabla_{\bar{\eta}_{non}} J_{non})^T \dot{\bar{\eta}}_{non} \right] \\ & + \frac{k}{2} \left[\left(\overline{e_{track}^1} \right)^T P_{Lyap}^1 \overline{e_{track}^1} + \left(\overline{e_{track}^1} \right)^T P_{Lyap}^1 \left(\overline{\dot{e}_{track}^1} \right) \right. \\ & \left. + \dots + \left(\overline{e_{track}^4} \right)^T P_{Lyap}^4 \overline{e_{track}^4} + \left(\overline{e_{track}^4} \right)^T P_{Lyap}^4 \left(\overline{\dot{e}_{track}^4} \right) \right] \\ & = \left[\nabla_t J_{non} + (\nabla_{\bar{\eta}_{non}} J_{non})^T \left(\bar{\rho}_{non_t}(t, \bar{\eta}_{non}, \overline{e_{track}}) + \varphi_{\bar{\eta}_{non}}(\bar{\theta}_{noise} + \bar{\theta}_{un}) \right) \right] \\ & + \left\{ \frac{k}{2\mathcal{E}} \left(\overline{e_{track}^1} \right)^T \left[P_{Lyap}^1 (A_c^1) + (A_c^1)^T P_{Lyap}^1 \right] \overline{e_{track}^1} + \dots \right. \\ & \left. + \frac{k}{2\mathcal{E}} \left(\overline{e_{track}^4} \right)^T \left[P_{Lyap}^4 (A_c^4) + (A_c^4)^T P_{Lyap}^4 \right] \overline{e_{track}^4} \right. \\ & \left. + \frac{k}{\mathcal{E}} \left(\bar{\theta}_{noise} + \bar{\theta}_{un} \right)^T \left[\left(\varphi_{\bar{\eta}_{lin}}^1 \right)^T P_{Lyap}^1 \overline{e_{track}^1} + \dots + \left(\varphi_{\bar{\eta}_{lin}}^4 \right)^T P_{Lyap}^4 \overline{e_{track}^4} \right] \right\} \\ & \leq \left[\nabla_t J_{non} + (\nabla_{\bar{\eta}_{non}} J_{non})^T \bar{\rho}_{non_t}(t, \bar{\eta}_{non}, \overline{e_{track}}) \right. \\ & \left. + \|\nabla_{\bar{\eta}_{non}} J_{non}\| \|\varphi_{\bar{\eta}_{non}}\| \|(\bar{\theta}_{noise} + \bar{\theta}_{un})\| \right] - \frac{k}{2\mathcal{E}} \left[\left\| \overline{e_{track}^1} \right\|^2 + \dots + \left\| \overline{e_{track}^4} \right\|^2 \right] \\ & \leq \left[\nabla_t J_{non} + (\nabla_{\bar{\eta}_{non}} J_{non})^T \bar{\rho}_{non_t}(t, \bar{\eta}_{non}, 0) \right] \\ & - (\nabla_{\bar{\eta}_{non}} J_{non})^T \bar{\rho}_{non_t}(t, \bar{\eta}_{non}, 0) \\ & + (\nabla_{\bar{\eta}_{non}} J_{non})^T \bar{\rho}_{non_t}(t, \bar{\eta}_{non}, \overline{e_{track}}) \\ & + \frac{k}{\mathcal{E}} \left[\|(\bar{\theta}_{noise} + \bar{\theta}_{un})\| \left(\|\varphi_{\bar{\eta}_{lin}}^1\| \|P_{Lyap}^1\| \left\| \overline{e_{track}^1} \right\| + \dots + \|\varphi_{\bar{\eta}_{lin}}^4\| \|P_{Lyap}^4\| \left\| \overline{e_{track}^4} \right\| \right) \right] \\ & + \|\nabla_{\bar{\eta}_{non}} J_{non}\| \|\varphi_{\bar{\eta}_{non}}\| \|(\bar{\theta}_{noise} + \bar{\theta}_{un})\| \\ & - \frac{k}{\mathcal{E}} \left[\frac{W_{lin}^1}{\gamma_{\max}(P_{Lyap}^1)} + \dots + \frac{W_{lin}^4}{\gamma_{\max}(P_{Lyap}^4)} \right] \\ & + \frac{121 k^2}{22 \mathcal{E}^2} \|\varphi_{\bar{\eta}_{lin}}^1\|^2 \|P_{Lyap}^1\|^2 \left\| \overline{e_{track}^1} \right\|^2 + \frac{1}{22} \|(\bar{\theta}_{noise} + \bar{\theta}_{un})\|^2 + \dots \\ & + \frac{121 k^2}{22 \mathcal{E}^2} \|\varphi_{\bar{\eta}_{lin}}^4\|^2 \|P_{Lyap}^4\|^2 \left\| \overline{e_{track}^4} \right\|^2 + \frac{1}{22} \|(\bar{\theta}_{noise} + \bar{\theta}_{un})\|^2 \end{aligned}$$

$$\begin{aligned}
&\leq -16\alpha_x J_{non} + \omega_{non3} \|\bar{\eta}_{non}\| M_{non} \|\overline{e_{track}}\| \\
&+ \omega_{non3} \|\bar{\eta}_{non}\| \|\varphi_{\eta_{non}}\| \|(\bar{\theta}_{noise} + \bar{\theta}_{un})\| - \frac{k}{\varepsilon} \frac{1}{\gamma_{max}^*} W_{lin} \\
&+ \frac{121 k^2}{22 \varepsilon^2} \|\varphi_{\xi_{lin}}^1\|^2 \|P_{Lyap}^1\|^2 \|\overline{e_{track}^1}\|^2 + \frac{1}{22} \|(\bar{\theta}_{noise} + \bar{\theta}_{un})\|^2 \\
&+ \dots + \frac{121 k^2}{22 \varepsilon^2} \|\varphi_{\xi_{lin}}^4\|^2 \|P_{Lyap}^4\|^2 \|\overline{e_{track}^4}\|^2 + \frac{1}{22} \|(\bar{\theta}_{noise} + \bar{\theta}_{un})\|^2 \\
&\leq -\left(16\alpha_x - \frac{121}{22} \left(\frac{\omega_{non3}}{\sqrt{\omega_{non1}}} \|\varphi_{\eta_{non}}\|\right)^2\right) (\sqrt{J_{non}})^2 \\
&+ 2 \left(\frac{\omega_{non3} M_{non}}{\sqrt{2\omega_{non1} k \gamma_{min}^*}}\right) \sqrt{J_{non}} \sqrt{k W_{lin}} \\
&- \left(\frac{1}{\varepsilon \gamma_{max}^*} - \frac{121 k}{22} \frac{\|\varphi_{\xi_{lin}}^1\|^2 \|P_{Lyap}^1\|^2}{\frac{1}{2} \varepsilon^2 \gamma_{min}(P_{Lyap}^1)} - \dots - \frac{121 k}{22} \frac{\|\varphi_{\xi_{lin}}^4\|^2 \|P_{Lyap}^4\|^2}{\frac{1}{2} \varepsilon^2 \gamma_{min}(P_{Lyap}^4)}\right) \\
&(\sqrt{k W_{lin}})^2 + \frac{5}{22} \|(\bar{\theta}_{noise} + \bar{\theta}_{un})\|^2 \tag{211} \\
&= -\left[\sqrt{J_{non}} \quad \sqrt{k W_{lin}}\right] H \begin{bmatrix} \sqrt{J_{non}} \\ \sqrt{k W_{lin}} \end{bmatrix} + \frac{5}{22} \|(\bar{\theta}_{noise} + \bar{\theta}_{un})\|^2
\end{aligned}$$

where the matrix H is positive definite, and

$$H(\varepsilon) \equiv \begin{bmatrix} H_{11} & H_{12} \\ H_{12} & H_{22} \end{bmatrix} \tag{212}$$

$$H_{11} = 16\alpha_x - \frac{121}{22} \frac{\omega_{non3}^2}{\omega_{non1}} \|\varphi_{\eta_{non}}\|^2 \tag{213}$$

$$H_{12} = -\left[\frac{\omega_{non3} M_{non}}{\sqrt{2k(\varepsilon) \omega_{non1} \gamma_{min}^*}}\right] \tag{214}$$

$$H_{22} = \frac{1}{\varepsilon \gamma_{max}^*} - \left(\frac{121}{22}\right) \frac{k(\varepsilon) \|\varphi_{\xi_{lin}}^1\|^2 \|P_{Lyap}^1\|^2}{\frac{1}{2} \varepsilon^2 \gamma_{min}(P_{Lyap}^1)} - \dots - \left(\frac{121}{22}\right) \frac{k(\varepsilon) \|\varphi_{\xi_{lin}}^m\|^2 \|P_{Lyap}^m\|^2}{\frac{1}{2} \varepsilon^2 \gamma_{min}(P_{Lyap}^m)} \tag{215}$$

i.e.

$$\dot{J}_{lin+non} \leq -\gamma_{min}(H) J_{lin+non} + \frac{5}{22} \|(\bar{\theta}_{noise} + \bar{\theta}_{un})\|^2 \tag{216}$$

where $\gamma_{min}(H)$ denotes the minimum eigenvalue of the matrix H .

Define

$$\alpha_s(\varepsilon) \equiv \frac{H_{11} + H_{22} - \left[(H_{11} - H_{22})^2 + 4H_{12}^2\right]^{1/2}}{4} \tag{217}$$

$$T \equiv 2\alpha_s(\varepsilon) \quad (218)$$

$$T_1 \equiv \frac{5}{22} \left(\sup_{t_0 \leq t \leq t} \|\bar{\theta}_{un} + \bar{\theta}_{noise}\| \right)^2 \quad (219)$$

$$T_2 \equiv \min \left\{ \omega_{non1}, \frac{k(\varepsilon)}{2} \gamma_{\min}^* \right\} \quad (220)$$

Applying (217) into (216) yields

$$\gamma_{\min}(H) = 2\alpha_s \quad (221)$$

$$\begin{aligned} \dot{J}_{lin+non} &\leq -2\alpha_s J_{lin+non} + \frac{5}{22} \|(\bar{\theta}_{noise} + \bar{\theta}_{un})\|^2 \\ &\leq -T \cdot T_2 \left(\|\bar{\eta}_{non}\|^2 + \|\bar{e}_{track}\|^2 \right) + \frac{5}{22} \|(\bar{\theta}_{noise} + \bar{\theta}_{un})\|^2 \end{aligned} \quad (222)$$

Define

$$\bar{e}_{track} \equiv \begin{bmatrix} \bar{e}_{track}^1 & \cdots & \bar{e}_{track}^4 \end{bmatrix}^T \equiv \begin{bmatrix} \bar{e}_1^1 & \bar{e}_{rem}^1 \end{bmatrix}^T, \bar{e}_{rem}^1 \in \mathfrak{R}^{d_o-1} \quad (223)$$

and get

$$\begin{aligned} \dot{J}_{lin+non} &\leq -T \cdot T_2 \left(\|\bar{\eta}_{non}\|^2 + \|\bar{e}_1^1\|^2 + \|\bar{e}_{rem}^1\|^2 \right) + \frac{5}{22} \|(\bar{\theta}_{noise} + \bar{\theta}_{un})\|^2 \end{aligned} \quad (224)$$

Next, we will prove the fact that the proposed feedback linearization control achieves the almost disturbance decoupling performance, and the globally exponential stability of the FLMA system in Appendix A. Therefore, the proposed robust tracking control (163) will indeed drive the tracking errors of the FLMA system into the global ultimate attractor.

Noting that we can extend above complete design process to obtain one more general significant theorem for general uncertain nonlinear control systems with disturbances as follows:

$$\begin{aligned} \begin{bmatrix} \dot{x}_1 & \cdots & \dot{x}_n \end{bmatrix}^T &= \begin{bmatrix} f_1(\bar{X}) & \cdots & f_n(\bar{X}) \end{bmatrix}^T \\ &+ \begin{bmatrix} \bar{g}_{fb_1}(\bar{X}) & \cdots & \bar{g}_{fb_m}(\bar{X}) \end{bmatrix} \begin{bmatrix} u_{fb_1}(\bar{X}) & \cdots & u_{fb_m}(\bar{X}) \end{bmatrix}^T \\ &+ \begin{bmatrix} \delta f_{un_1}(\bar{X}) & \cdots & \delta f_{un_n}(\bar{X}) \end{bmatrix}^T + \sum_{j=1}^p \bar{q}_j^* \theta_{noise_j} \end{aligned} \quad (225)$$

$$\begin{bmatrix} y_{o1}(\bar{X}) & \cdots & y_{om}(\bar{X}) \end{bmatrix}^T = \begin{bmatrix} \sigma_{o1}(\bar{X}) & \cdots & \sigma_{om}(\bar{X}) \end{bmatrix}^T \quad (226)$$

i.e.,

$$\dot{\bar{X}}(t) = \bar{f}(\bar{X}(t)) + \bar{g}_{fb}(\bar{X}(t)) \bar{u}_{fb} + \delta \bar{f}_{un} + \sum_{j=1}^p \bar{q}_j^* \theta_{noise_j} \quad (227)$$

$$\bar{y}_o(t) = \bar{\sigma}_o(\bar{X}(t)) \quad (228)$$

where $\bar{u}_{fb} \equiv [u_{fb_1} u_{fb_2} \cdots u_{fb_m}]^T$, $\bar{y}_o \equiv [y_{o1} y_{o2} \cdots y_{om}]^T$ denote the input and output, respectively, $\bar{X}(t) \equiv [x_1(t) x_2(t) \cdots x_n(t)]^T$ is the state variable, $\bar{\theta}_{noise} \equiv [\theta_{noise_1}(t) \theta_{noise_2}(t) \cdots \theta_{noise_p}(t)]^T$ is the noise vector, \bar{q}_j^* denotes the noise_adjoint vector. Assume $\bar{f} \equiv [f_1 f_2 \cdots f_n]^T$, $\bar{g}_{fb} \equiv [\bar{g}_{fb_1} \bar{g}_{fb_2} \cdots \bar{g}_{fb_m}]$ and $\bar{\sigma}_o \equiv [\sigma_{o1} \sigma_{o2} \cdots \sigma_{om}]^T$ to be continuous functions, and $\delta \bar{f}_{un}$ to be the matched uncertainty vector term $\delta \bar{f}_{un} \equiv \sum_{j=1}^p \bar{q}_j^* \theta_{un_j}$, where $\bar{\theta}_{un} \equiv [\theta_{un_1}(t) \theta_{un_2}(t) \cdots \theta_{un_p}(t)]^T$ is defined to be the uncertainty vector.

Assumption 2. The following inequality holds:

$$\|\bar{\rho}_{non_t}(t, \bar{\eta}_{non}, \bar{e}_{track}) - \bar{\rho}_{non_t}(t, \bar{\eta}_{non}, 0)\| \leq M_{non} (\|\bar{e}_{track}\|) \quad (229)$$

where $M_{non} > 0$ and $\bar{\rho}_{non_t}(t, \bar{\eta}_{non}, \bar{e}_{track}) \equiv \bar{\rho}_{non}(\bar{\xi}_{lin}, \bar{\eta}_{non})$.

Then the nominal system will be

$$\dot{\bar{X}}(t) = \bar{f}(\bar{X}(t)) + \bar{g}_{fb}(\bar{X}(t)) \bar{u}_{fb} \quad (230)$$

$$\bar{y}_o(t) = \bar{\sigma}_o(\bar{X}(t)) \quad (231)$$

and it is assumed to have the vector relative frequency $\{d_{o1}, d_{o2}, \dots, d_{om}\}$ [39]:

<i>The following condition holds:

$$L_{\bar{g}_{fb_j}} L_{\bar{f}}^k \sigma_{oi}(\bar{X}) = 0 \quad (232)$$

for all $1 \leq i, j \leq m$, $k < d_{oi} - 1$, where the symbol L is the Lie operator.

<ii>The square matrix

$$A \equiv \begin{bmatrix} L_{\bar{g}_{fb_1}} L_{\bar{f}}^{d_{o1}-1} \sigma_{o1}(\bar{X}) & \cdots & L_{\bar{g}_{fb_m}} L_{\bar{f}}^{d_{o1}-1} \sigma_{o1}(\bar{X}) \\ \vdots & & \vdots \\ L_{\bar{g}_{fb_1}} L_{\bar{f}}^{d_{om}-1} \sigma_{om}(\bar{X}) & \cdots & L_{\bar{g}_{fb_m}} L_{\bar{f}}^{d_{om}-1} \sigma_{om}(\bar{X}) \end{bmatrix} \quad (233)$$

has nonsingular property. The norms of pre-specified tracking signals y_{track}^i , $1 \leq i \leq m$ and its first d_{oi} derivatives are bounded by positive constants B_{track}^i as:

$$\| [y_{track}^i, y_{track}^{i(1)}, \dots, y_{track}^{i(d_{oi})}] \| \leq B_{track}^i, 1 \leq i \leq m \quad (234)$$

and the spanning distribution

$$G \equiv span\{\bar{g}_{fb_1}, \bar{g}_{fb_2}, \dots, \bar{g}_{fb_m}\} \quad (235)$$

is involutive. Then the mapping $\varphi: \mathfrak{X}^n \rightarrow \mathfrak{X}^n$ defined as

$$\begin{aligned} \bar{\xi}_{lin_i} &\equiv \left[\xi_{lin_{-1}}^i \quad \cdots \quad \xi_{lin_{-d_{oi}}}^i \right]^T \equiv \left[\varphi_{lin_{-1}}^i \quad \cdots \quad \varphi_{lin_{-d_{oi}}}^i \right]^T \\ &\equiv \left[L_f^0 \sigma_{oi}(\bar{X}) \quad \cdots \quad L_f^{d_{oi}-1} \sigma_{oi}(\bar{X}) \right]^T, d_o \equiv d_{o1} + d_{o2} + \cdots + d_{om} \end{aligned} \quad (236)$$

$$\varphi_{non_k}(\bar{X}(t)) \equiv \eta_{non_k}(t), k = d_o + 1, d_o + 2, \dots, n \quad (237)$$

and

$$L_{g_{\rho_j}} \varphi_{non_k}(\bar{X}(t)) = 0, k = d_o + 1, d_o + 2, \dots, n, 1 \leq j \leq m \quad (238)$$

is an one-to-one and onto, infinitely continuous and differentiable function according to reference [39].

Let J_{non} and W_{lin} be the Lyapunov functions of nonlinear subsystem and linear subsystem, respectively and then combine these Lyapunov functions to be a composite Lyapunov function $J_{lin+non}$ as follows:

$$J_{lin+non} \equiv J_{non} + k(\varepsilon)W_{lin} \quad (239)$$

$$W_{lin} = W_{lin}^1 \left(\overline{e_{track}^1} \right) + \cdots + W_{lin}^m \left(\overline{e_{track}^m} \right) \quad (240)$$

$$W_{lin}^i \left(\overline{e_{track}^i} \right) \equiv \frac{1}{2} \overline{e_{track}^i}^T P_{Lyap}^i \overline{e_{track}^i} \quad (241)$$

Theorem 1. A differentiable and infinitely continuous function $J_{non} : \mathfrak{R}^{n-r} \rightarrow \mathfrak{R}^+$ for transformed nonlinear subsystem can be found to make the following three inequalities hold:

$$(a) \omega_{non1} \|\bar{\eta}_{non}\|^2 \leq J_{non}(\bar{\eta}_{non}) \leq \omega_{non2} \|\bar{\eta}_{non}\|^2 \quad (242)$$

$$(b) \nabla_t J_{non} + (\nabla_{\bar{\eta}_{non}} J_{non})^T \bar{\rho}_{non}(t, \bar{\eta}_{non}, 0) \leq -16\alpha_x J_{non} \quad (243)$$

$$(c) \|\nabla_{\bar{\eta}_{non}} J_{non}\| \leq \omega_{non3} \|\bar{\eta}_{non}\|, \omega_{non3} > 0 \quad (244)$$

Design the robust and tracking controller to be

$$\bar{u}_{\rho_b} = A^{-1} \{-\bar{u}_b + \bar{u}_v\} \quad (245)$$

$$\bar{u}_b \equiv [u_{b1} \quad u_{b2} \quad \cdots \quad u_{bm}]^T \equiv \left[L_f^{d_{o1}} \sigma_{o1} \quad L_f^{d_{o2}} \sigma_{o2} \quad \cdots \quad L_f^{d_{om}} \sigma_{om} \right]^T \quad (246)$$

$$\bar{u}_v \equiv [u_{v1} \quad u_{v2} \quad \cdots \quad u_{vm}]^T \quad (247)$$

$$\begin{aligned} u_{vi} &\equiv y_{track}^{i(d_{oi})} - \varepsilon^{-d_{oi}} \alpha_1^i \left[L_f^0 \sigma_{oi}(\bar{X}) - y_{track}^i \right] \\ &- \varepsilon^{1-d_{oi}} \alpha_2^i \left[L_f^1 \sigma_{oi}(\bar{X}) - y_{track}^{i(1)} \right] - \cdots - \varepsilon^{-1} \alpha_{d_{oi}}^i \left[L_f^{d_{oi}-1} \sigma_{oi}(\bar{X}) - y_{track}^{i(d_{oi}-1)} \right] \end{aligned} \quad (248)$$

Then the nonlinear system possesses the almost disturbance decoupling performance with the globally exponential stability:

$$H(\varepsilon) \equiv \begin{bmatrix} H_{11} & H_{12} \\ H_{12} & H_{22} \end{bmatrix} \quad (249)$$

$$H_{11} = 16\alpha_x - \frac{121}{22} \frac{\omega_{non3}^2}{\omega_{non1}} \|\varphi_{\bar{n}_{non}}\|^2 \quad (250)$$

$$H_{12} = - \left[\frac{w_{non3} M_{non}}{\sqrt{2k(\varepsilon) w_{non1} \gamma_{min}^*}} \right] \quad (251)$$

$$H_{22} = \frac{1}{\varepsilon \gamma_{max}^*} - \left(\frac{121}{22} \right) \frac{k(\varepsilon) \|\varphi_{\xi_{lin}}^1\|^2 \|P_{Lyap}^1\|^2}{1/2 \varepsilon^2 \gamma_{min}(P_{Lyap}^1)} - \dots - \left(\frac{121}{22} \right) \frac{k(\varepsilon) \|\varphi_{\xi_{lin}}^m\|^2 \|P_{Lyap}^m\|^2}{1/2 \varepsilon^2 \gamma_{min}(P_{Lyap}^m)} \quad (252)$$

$$\alpha_s(\varepsilon) \equiv \frac{H_{11} + H_{22} - [(H_{11} - H_{22})^2 + 4H_{12}^2]^{1/2}}{4} \quad (253)$$

$$T \equiv 2\alpha_s(\varepsilon) \quad (254)$$

$$T_1 \equiv \frac{m+1}{22} \left(\sup_{t_0 \leq \tau \leq t} \|\bar{\theta}_{un} + \bar{\theta}_{noise}\| \right)^2 \quad (255)$$

$$T_2 \equiv \min \left\{ \omega_{non1}, \frac{k(\varepsilon)}{2} \gamma_{min}^* \right\} \quad (256)$$

$$\varphi_{\xi_{lin}}^j(\varepsilon) \equiv \begin{bmatrix} \varepsilon \left(\frac{\partial}{\partial \bar{X}} \sigma_{oi} \right) \bar{q}_1^* & \dots & \varepsilon \left(\frac{\partial}{\partial \bar{X}} \sigma_{oi} \right) \bar{q}_p^* \\ \vdots & & \vdots \\ \varepsilon^{d_{oi}} \left(\frac{\partial}{\partial \bar{X}} L_f^{d_{oi}-1} \sigma_{oi} \right) \bar{q}_1^* & \dots & \varepsilon^{d_{oi}} \left(\frac{\partial}{\partial \bar{X}} L_f^{d_{oi}-1} \sigma_{oi} \right) \bar{q}_p^* \end{bmatrix} \quad (257)$$

$$\varphi_{\bar{n}_{non}}(\varepsilon) \equiv \begin{bmatrix} \left(\frac{\partial}{\partial \bar{X}} \varphi_{non-d_o+1} \right) \bar{q}_1^* & \dots & \left(\frac{\partial}{\partial \bar{X}} \varphi_{non-d_o+1} \right) \bar{q}_p^* \\ \vdots & & \vdots \\ \left(\frac{\partial}{\partial \bar{X}} \varphi_{non-n} \right) \bar{q}_1^* & \dots & \left(\frac{\partial}{\partial \bar{X}} \varphi_{non-n} \right) \bar{q}_p^* \end{bmatrix} \quad (258)$$

where the matrix H is positive definite, and the continuous function $k(\varepsilon): \mathfrak{R}^+ \rightarrow \mathfrak{R}^+$ satisfies $\lim_{\varepsilon \rightarrow 0} k(\varepsilon) = 0$ and

$$\lim_{\varepsilon \rightarrow 0} \frac{\varepsilon}{k(\varepsilon)} = 0 \quad (259)$$

Moreover, the desired tracking errors can be exponentially reduced by adjusting the parameter $T \cdot T_2 > 1$ with the convergence rate formula

$$\frac{T \cdot T_2}{\Delta_{max}} \quad (260)$$

$$\Delta_{max} \equiv \max \left\{ \omega_{non2}, \frac{k}{2} \gamma_{max}^* \right\} \quad (261)$$

and the desired tracking errors of control system are exponentially attracted into a global final attractor B_z with the convergence radius formula

$$z = \sqrt{\frac{T_1}{T \cdot T_2}} \quad (262)$$

To effectively build robust and tracking controller, a significant algorithm of FLMA is summarized as follows, and then a powerful Python software system of controller design is constructed in the next section according to this proposed algorithm.

(Step 1) Obtain the vector relative frequency d_{o1}, \dots, d_{om} according to the given outputs $\sigma_{o1}, \dots, \sigma_{om}$.

(Step 2) Appropriately construct the one-to-one and onto, infinitely continuous and differentiable function ϕ based on (123)~(127).

(Step 3) From (162) and (178), appropriately choose parameters $\alpha_{d_{oi}}^i$ such that A_c^i are Hurwitz matrices with stable eigenvalues and obtain the positive definite $P_{Lyap}^i > 0$ of the Lyapunov equation with the aid of Matlab toolbox.

(Step 4) Choose the Lyapunov function J_{non} to meet the requirements (184) and (198)~(200). If the vector relative frequency is equal to the system dimension, i.e. $d_{o1} + \dots + d_{om} = n$, then this step will be omitted and directly go to (Step 5).

(Step 5) From (212)~(215), (217)~(220), appropriately design parameters $k, \alpha_s(\varepsilon), \varepsilon$ to meet $T \cdot T_2 > 1$. It is worth noting that if the value of $T \cdot T_2$ is larger, the convergence rate is faster.

(Step 6) Finally, the robust and tracking controller can be built by (163).

4. Simulations of the FLMA System

It can be verified that the related requirements of Theorem 1 hold if we choose $\varepsilon = 0.01$, $k(\varepsilon) = 2000\sqrt{\varepsilon}$, $d_{o1} = d_{o2} = d_{o3} = d_{o4} = 1$, $\alpha_s = 1$, $H_{11} = 2$, $T = 2$, $T_2 = 1$, $H_{22} = 100\varepsilon^{-1}$, $H_{12} = -0.1\varepsilon^{-1/4}$. Hence the robust and tracking controller will make the tracking errors converge to the globally final attractor by Theorem 1. The real tracking errors of the FLMA system (epsilon=0.01) are plotted in Figure 2. Therefore, the designed controller can indeed make the outputs track the pre-specified signals $y_{track}^1 = y_{track}^2 = y_{track}^3 = y_{track}^4 = \pi/6$. From (260)~(261) and Figure 2~Figure 3, it is obvious to see that the convergent rate of tracking error with smaller epsilon is better than a larger epsilon. Moreover, the dynamic trajectories show the overall tracking errors "before", "on" and "after" entering the globally final attractor in the positive z direction for Figure 4, Figure 5 and Figure 6, respectively, where the length of the arrow denotes the convergence-radius of the globally final attractor. Other individual tracking errors of the output 1~output 4 are shown in positive x direction, negative x direction, positive y direction and negative y direction for Figure 4, Figure 5 and Figure 6, respectively.

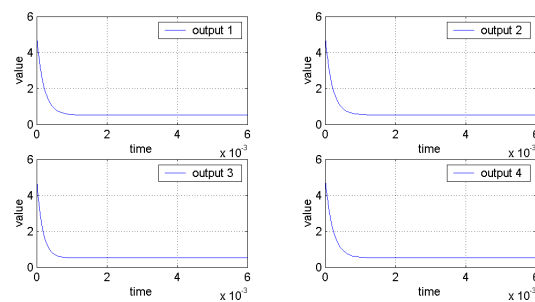


Figure 2. The output trajectories for $\varepsilon = 0.01$.

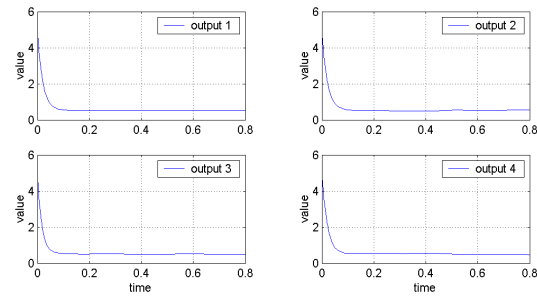


Figure 3. The output trajectories for $\varepsilon = 1$.

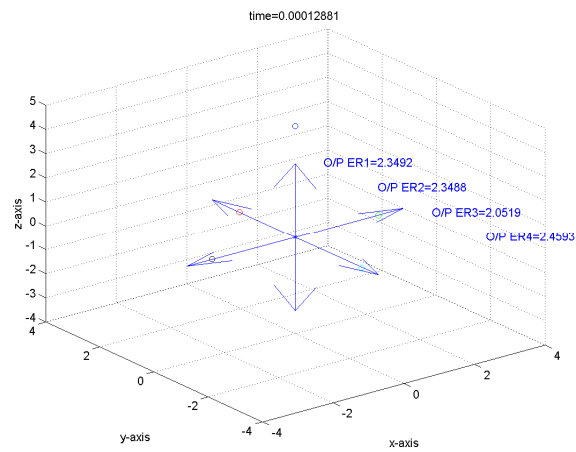


Figure 4. Tracking error before entering the global final attractor.

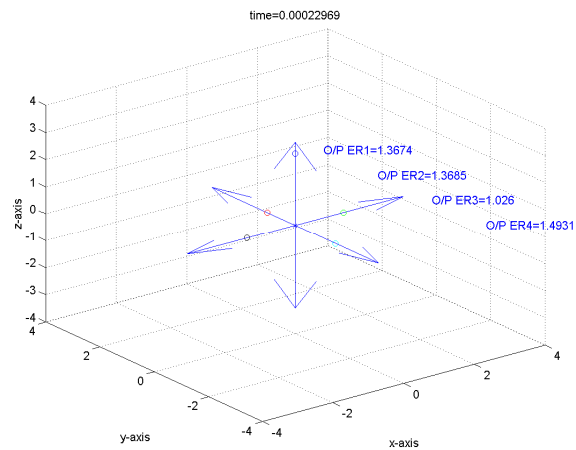


Figure 5. Tracking error on entering the global final attractor.

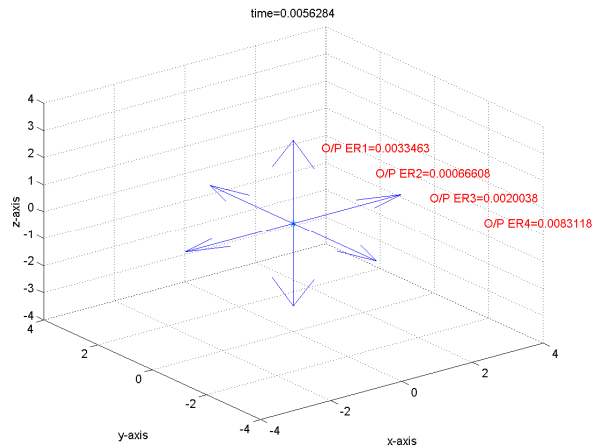


Figure 6. Tracking error after entering the global final attractor.

5. Comparisons to Traditional Approaches

In this section, we will compare the performance of proposed approach with traditional fuzzy approach [41] and the singular perturbation method with high-gain feedback [38].

Figure 7 is the general structure of traditional fuzzy approach whose input variables of the IF-THEN rules are assigned to be the tracking error $e(t)$ and its time derivative $\dot{e}(t)$. The output variable is the fuzzy control u_{fuzzy} . For easy calculation, the desired membership functions of $e_{track}(t)$, $\dot{e}_{track}(t)$ and u_{fuzzy} are assigned to be the triangular shape functions as shown in Figure 8~Figure 10. The desired fuzzy control rule base for u_{fuzzy} is constructed in Table 1. The rule base, fuzzy inference engine and defuzzifier adopt the standard Macvicar-Whelan rule base, the Mamdani method and the centroid method, respectively.

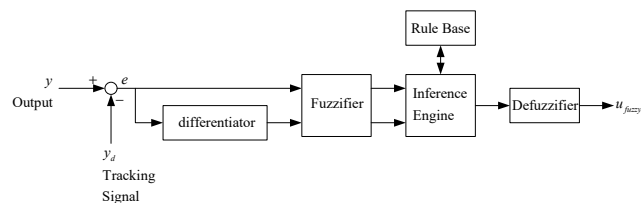


Figure 7. General structure of traditional fuzzy approach.

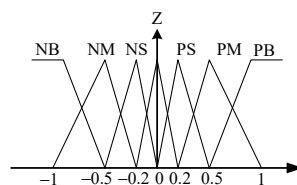


Figure 8. Triangular shape membership functions for $e(t)$.

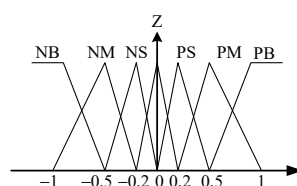


Figure 9. Triangular shape membership functions for $\dot{e}(t)$.

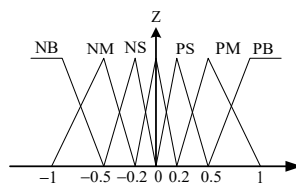


Figure 10. Triangular shape membership functions for u_{fuzzy} .

Table 1. MACVICAR-WHELAN fuzzy control rule base.

u_{fuzzy}		$e_{track}(t)$						
		NB	NM	NS	ZE	PS	PM	PB
$\dot{e}_{track}(t)$	NB	PB	PB	PB	PB	PM	PS	ZE
	NM	PB	PB	PB	PM	PS	ZE	NS
	NS	PB	PB	PM	PS	ZE	NS	NM
	ZE	PB	PM	PS	ZE	NS	NM	NB
	PS	PM	PS	ZE	NS	NM	NB	NB
	PM	PS	ZE	NS	NM	NB	NB	NB
	PB	ZE	NS	NM	NB	NB	NB	NB

With the aid of Matlab fuzzy toolbox, comparative tracking error responses of the proposed approach and traditional fuzzy controller design for the FLMA are shown in Figure 11 ~ Figure 14. From Figure 11 ~ Figure 14, it is obvious to see that the convergence rate of the proposed approach is faster than the traditional fuzzy approach.

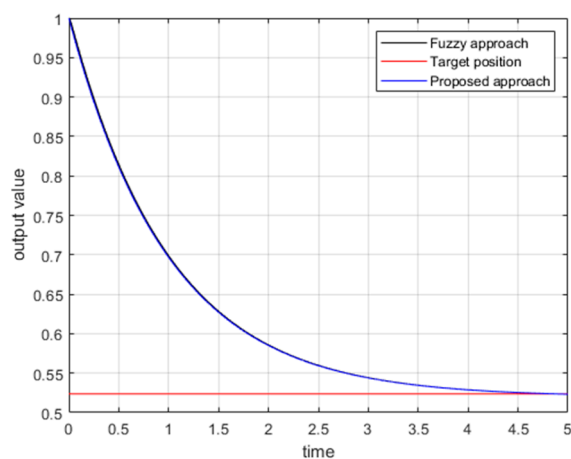


Figure 11. The output tracking error for the output 1.

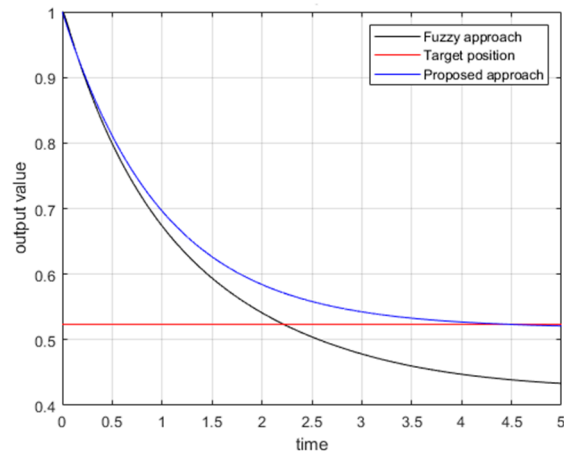


Figure 12. The output tracking error for the output 2.

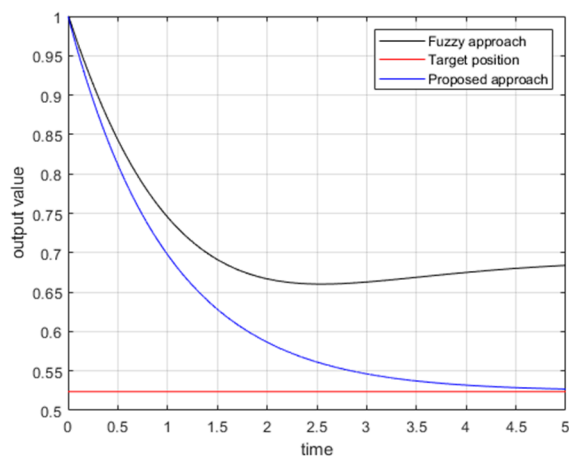


Figure 13. The output tracking error for the output 3.

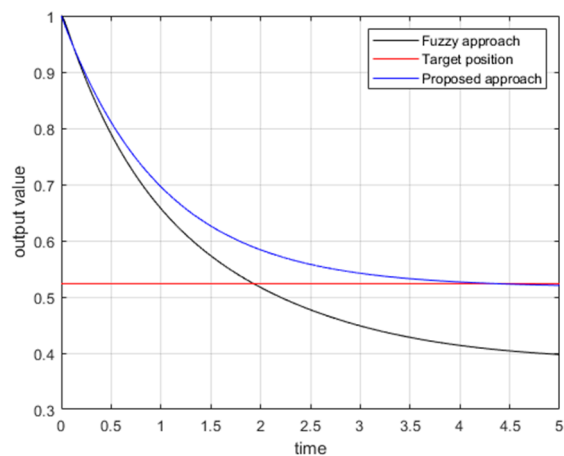


Figure 14. The output tracking error for the output 4.

Following the second comparative example, we will make some comparison between the proposed approach and the famous singular perturbation method [37,38]. The sufficient condition in [37,38] needs that the nonlinearity multiplied by the disturbance meets the structural triangle criterion.

References [37,38] had exploited the fact that the following system cannot achieve the almost disturbance decoupling performance:

$$\begin{bmatrix} \dot{x}_1(t) \\ \dot{x}_2(t) \end{bmatrix} = \begin{bmatrix} \tan^{-1}(x_2) \\ 0 \end{bmatrix} + \begin{bmatrix} 0 \\ 1 \end{bmatrix} u_{fb} + \begin{bmatrix} 1 \\ 0 \end{bmatrix} w_{noise}(t) \quad (263)$$

$$y_{o1} = x_1 \equiv \sigma_{o1}, w_{noise}(t) = 0.1 \sin t \quad (264)$$

It is easy to derive the following items: $L_f^0 \sigma_{o1} = \sigma_{o1} = x_1$, $L_{g_b} L_f^0 \sigma_{o1} = 0$, $L_f^1 \sigma_{o1} = \tan^{-1}(x_2)$, $L_{g_b} L_f^1 \sigma_{o1} = \frac{1}{1+x_2^2}$ and

$$\tilde{g}_{fb} \equiv \begin{bmatrix} 0 \\ \frac{1}{L_{g_b} L_f^1 \sigma_{o1}} \end{bmatrix} = \begin{bmatrix} 0 \\ 1+x_2^2 \end{bmatrix} \quad (265)$$

Hence the sufficient condition of [37][38] is not satisfied since \tilde{g} is not complete, and then the almost disturbance decoupling problem cannot be not solved. On the contrary, this almost disturbance decoupling problem can be solved via the proposed approach by the controller

$$u_{fb} = (1+x_2^2)[- \sin t - 52(x_1 - \sin t + \tan^{-1} x_2 - \cos t)] \quad (266)$$

The output response of the nonlinear system for (263) is shown in Figure 15. Therefore, the designed controller can indeed make the output track the pre-specified signals $y_{track}^1 = \sin t$ and achieve the almost disturbance decoupling performance.

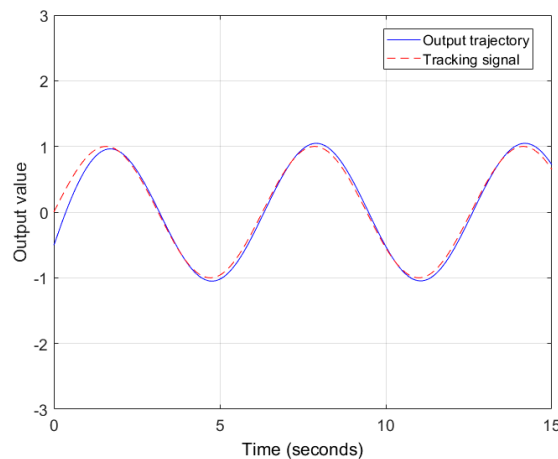


Figure 15. The output trajectory of feedback-controlled system for (263).

6. Conclusion

Continuous spreading COVID-19 virus stimulates us to design the robust controller of the highly nonlinear FLMA by the feedback linearized approach that possesses almost disturbance decoupling performance taking the place of the traditional posture-energy approach and avoiding torque chattering change behaviour in the swing-up space, and other globally exponential stability performance without solving the famous Hamilton-Jacobi equation. The disturbance has a sensitive effect on FLMA and then this article addresses stricter disturbance requirements including absolute value error, integration error and input-to-state stable condition.

This study derives successfully the nonlinear convergence rate formula of the FLMA and the related convergence radius of the globally final attractor. Moreover, in order to clearly show that dynamic trajectories of the output tracking-errors for the nonlinear FLMA system converge to the global final attractor, one Matlab software are completely designed to demonstrate the tracking-error trajectories before, on and after entering the globally final attractor.

The simulation results of two demonstrative examples show that the convergence rate using proposed controller is faster than using traditional fuzzy controller, and superior to the traditional singular perturbation approach.

Supplementary Materials:

Author Contributions: Conceptualization, Kuang-Hui Chi; methodology, Chung-Cheng Chen; software, Yung-Feng Hsiao; validation, Yung-Feng Hsiao; formal analysis, Yung-Feng Hsiao; investigation, Yung-Feng Hsiao; resources, Kuang-Hui Chi; data curation, Kuang-Hui Chi; writing—original draft preparation, Chung-Cheng Chen; writing—review and editing, Kuang-Hui Chi and Yung-Feng Hsiao; visualization, Kuang-Hui Chi; supervision, Chung-Cheng Chen; project administration, Kuang-Hui Chi and Chung-Cheng Chen.

Funding:

Institutional Review Board Statement:

Informed Consent Statement:

Data Availability Statement: No new data were created or analyzed in this study. Data sharing is not applicable to this article.

Acknowledgments:

Conflicts of Interest: The authors declare no conflicts of interest.

Appendix A

In Appendix A, we will prove that the nonlinear FLMA system with the proposed control can achieve the three almost all disturbance decoupling performances, the convergent radius formula and the globally exponential stability. First, applying (224) easily gets

In Appendix A, we will prove that the nonlinear FLMA system with the proposed control can achieve the three almost all disturbance decoupling performances, the convergent radius formula and the globally exponential stability. First, applying (224) easily gets

$$\begin{aligned}
 & \dot{J}_{lin+non} + T \cdot T_2 \left\| \bar{e}_1^- \right\|^2 \\
 & \leq -T \cdot T_2 \left(\left\| \bar{\eta}_{non} \right\|^2 + \left\| \bar{e}_{rem}^- \right\|^2 \right) + \frac{5}{22} \left\| (\bar{\theta}_{noise} + \bar{\theta}_{un}) \right\|^2 \leq \frac{5}{22} \left\| (\bar{\theta}_{noise} + \bar{\theta}_{un}) \right\|^2 \\
 & \dot{J}_{lin+non} + T \cdot T_2 \left\| \bar{e}_1^- \right\|^2 \\
 & \leq -T \cdot T_2 \left(\left\| \bar{\eta}_{non} \right\|^2 + \left\| \bar{e}_{rem}^- \right\|^2 \right) + \frac{5}{22} \left\| (\bar{\theta}_{noise} + \bar{\theta}_{un}) \right\|^2 \\
 & \leq \frac{5}{22} \left\| (\bar{\theta}_{noise} + \bar{\theta}_{un}) \right\|^2
 \end{aligned} \tag{A.1}$$

i.e.

$$\dot{J}_{lin+non} + T \cdot T_2 \left\| \bar{e}_1 \right\|^2 \leq \frac{5}{22} \left\| (\bar{\theta}_{noise} + \bar{\theta}_{un}) \right\|^2 \quad (\text{A.2})$$

Integrate both sides of the inequality (A.2) to get

$$J_{lin+non}(t) - J_{lin+non}(t_0) + T \cdot T_2 \int_{t_0}^t (y_{oi}(\tau) - y_{track}^1(\tau))^2 d\tau \leq \frac{5}{22} \int_{t_0}^t \left\| (\bar{\theta}_{noise} + \bar{\theta}_{un}) \right\|^2 d\tau \quad (\text{A.3})$$

i.e.

$$T \cdot T_2 \int_{t_0}^t (y_{oi}(\tau) - y_{track}^1(\tau))^2 d\tau \leq J_{lin+non}(t_0) + \frac{5}{22} \int_{t_0}^t \left\| (\bar{\theta}_{noise} + \bar{\theta}_{un}) \right\|^2 d\tau \quad (\text{A.4})$$

Therefore,

$$\int_{t_0}^t (y_{oi}(\tau) - y_{track}^1(\tau))^2 d\tau \leq \frac{J_{lin+non}(t_0)}{T \cdot T_2} + \frac{5}{22 \cdot T \cdot T_2} \int_{t_0}^t \left\| (\bar{\theta}_{noise} + \bar{\theta}_{un}) \right\|^2 d\tau \quad (\text{A.5})$$

Similarly, we can extend above result to be

$$\begin{aligned} & \int_{t_0}^t (y_{oi}(\tau) - y_{track}^i(\tau))^2 d\tau \\ & \leq \frac{J_{lin+non}(t_0)}{T \cdot T_2} + \frac{5}{22 \cdot T \cdot T_2} \int_{t_0}^t \left\| (\bar{\theta}_{noise} + \bar{\theta}_{un}) \right\|^2 d\tau, 2 \leq i \leq 4 \end{aligned} \quad (\text{A.6})$$

and then we can conclude that the third almost disturbance decoupling requirement is achieved. Next, we will achieve the first almost disturbance decoupling performance. (222) can be rewritten as

$$\begin{aligned} \dot{J}_{lin+non} & \leq -2\alpha_s J_{lin+non} + \frac{5}{22} \left\| (\bar{\theta}_{noise} + \bar{\theta}_{un}) \right\|^2 \\ & \leq -T \cdot T_2 \left(\left\| \bar{\eta}_{non} \right\|^2 + \left\| \bar{e}_{track} \right\|^2 \right) + \frac{5}{22} \left\| (\bar{\theta}_{noise} + \bar{\theta}_{un}) \right\|^2 \end{aligned} \quad (\text{A.7})$$

Let

$$\left\| \bar{y}_{track-total} \right\|^2 \equiv \left\| \bar{e}_{track} \right\|^2 + \left\| \bar{\eta}_{non} \right\|^2 \quad (\text{A.8})$$

Combining (A.7) and (A.8) yields

$$\dot{J}_{lin+non} \leq -T \cdot T_2 \left\| \bar{y}_{track-total} \right\|^2 + \frac{5}{22} \left\| (\bar{\theta}_{noise} + \bar{\theta}_{un}) \right\|^2 \quad (\text{A.9})$$

Then

$$\dot{J}_{lin+non} \leq -(T \cdot T_2 - 1) \left\| \bar{y}_{track-total} \right\|^2 - \left\| \bar{y}_{track-total} \right\|^2 + \frac{5}{22} \left\| (\bar{\theta}_{noise} + \bar{\theta}_{un}) \right\|^2 \quad (\text{A.10})$$

Therefore, the state trajectory lying in the outside of the global ultimate attractor is described by

$$-\left\| \bar{y}_{track-total} \right\|^2 + \frac{5}{22} \left\| (\bar{\theta}_{noise} + \bar{\theta}_{un}) \right\|^2 < 0 \quad (\text{A.11})$$

Then

$$\dot{J}_{lin+non} \leq -(T \cdot T_2 - 1) \left\| \bar{y}_{track-total} \right\|^2 \quad (\text{A.12})$$

From (181), (198), (201) and (204), we get

$$\begin{aligned}
J_{lin+non} &= J_{non} + k(\varepsilon) \left(W_{lin}^1 + W_{lin}^2 + W_{lin}^3 + W_{lin}^4 \left(\overline{e_{track}^4} \right) \right) \\
&\leq \omega_{non2} \|\bar{\eta}_{non}\|^2 + k \frac{1}{2} \left\{ \gamma_{\max} (P_{Lyap}^1) \left\| \overline{e_{track}^1} \right\|^2 + \dots + \gamma_{\max} (P_{Lyap}^4) \left\| \overline{e_{track}^4} \right\|^2 \right\} \\
&\leq \omega_{non2} \|\bar{\eta}_{non}\|^2 + k \frac{1}{2} \gamma_{\max}^* \left\{ \left\| \overline{e_{track}^1} \right\|^2 + \dots + \left\| \overline{e_{track}^4} \right\|^2 \right\} \\
&\leq \omega_{non2} \|\bar{\eta}_{non}\|^2 + k \frac{1}{2} \gamma_{\max}^* \left\| \overline{e_{track}} \right\|^2
\end{aligned} \tag{A.13}$$

Define $\Delta_{\max} \equiv \max \left\{ \omega_{non2}, \frac{k}{2} \gamma_{\max}^* \right\}$ and we can get

$$J_{lin+non} \leq \Delta_{\max} \left(\left\| \bar{y}_{track-total} \right\|^2 \right) \tag{A.14}$$

Similarly, we can achieve

$$\begin{aligned}
J_{lin+non} &= J_{non} + k(\varepsilon) \left(W_{lin}^1 + W_{lin}^2 + W_{lin}^3 + W_{lin}^4 \right) \\
&\geq \omega_{non1} \|\bar{\eta}_{non}\|^2 + k \frac{1}{2} \left\{ \gamma_{\min} (P_{Lyap}^1) \left\| \overline{e_{track}^1} \right\|^2 + \dots + \gamma_{\min} (P_{Lyap}^4) \left\| \overline{e_{track}^4} \right\|^2 \right\} \\
&\geq \omega_{non1} \|\bar{\eta}_{non}\|^2 + k \frac{1}{2} \gamma_{\min}^* \left\{ \left\| \overline{e_{track}^1} \right\|^2 + \dots + \left\| \overline{e_{track}^4} \right\|^2 \right\} \\
&\geq \omega_{non1} \|\bar{\eta}_{non}\|^2 + k \frac{1}{2} \gamma_{\min}^* \left\| \overline{e_{track}} \right\|^2
\end{aligned} \tag{A.15}$$

Define $\Delta_{\min} \equiv \min \left\{ \omega_{non1}, \frac{k}{2} \gamma_{\min}^* \right\}$ and we can obtain

$$\Delta_{\min} \left(\left\| \bar{y}_{track-total} \right\|^2 \right) \leq J_{lin+non} \tag{A.16}$$

Combining (A.14) and (A.16) gets

$$\Delta_{\min} \left(\left\| \bar{y}_{track-total} \right\|^2 \right) \leq J_{lin+non} \leq \Delta_{\max} \left(\left\| \bar{y}_{track-total} \right\|^2 \right) \tag{A.17}$$

From (A.11)-(A.12) and (A.17) and the input-to-state stable theorem [40], we can conclude that the first almost disturbance decoupling requirement is achieved. Next, we will achieve the first almost disturbance decoupling performance. Combining (A.7), (A.8), (A.17) and (219) gets

$$\dot{J}_{lin+non} \leq -\frac{T \cdot T_2}{\Delta_{\max}} J_{lin+non} + T_1 \tag{A.18}$$

Applying the comparison theorem to (A.18) yields

$$J_{lin+non}(t) \leq J_{lin+non}(t_0) e^{-\frac{T \cdot T_2}{\Delta_{\max}}(t-t_0)} + \frac{\Delta_{\max} T_1}{T \cdot T_2}, t \geq t_0 \tag{A.19}$$

Then we can get

$$\left| y_{o1}(t) - y_{track}^1(t) \right| \leq \sqrt{\frac{2J_{lin+non}(t_0)}{k \gamma_{\min}^*}} e^{-\frac{T \cdot T_2}{2\Delta_{\max}}(t-t_0)} + \sqrt{\frac{2\Delta_{\max} T_1}{k \gamma_{\min}^* T \cdot T_2}} \tag{A.20}$$

and

$$|y_{oi}(t) - y_{track}^i(t)| \leq \sqrt{\frac{2J_{lin+non}(t_0)}{k\gamma_{min}^*}} e^{-\frac{T \cdot T_2}{2\Delta_{max}}(t-t_0)} + \sqrt{\frac{2\Delta_{max}T_1}{k\gamma_{min}^* T \cdot T_2}}, \quad (A.21)$$

$$2 \leq i \leq 4$$

Observing (A.21) verifies the second almost disturbance decoupling requirement and the convergence rate of tracking errors is $T \cdot T_2 / \Delta_{max}$. It is obvious to see that we can change the value of $T \cdot T_2$ to adjust the convergence rate. Moreover, from (A.7), (A.8) and (219), we get

$$\dot{J}_{lin+non} \leq -T \cdot T_2 \left(\|\bar{y}_{track-total}\|^2 \right) + T_1 \quad (A.22)$$

Considering the output trajectory for $\|\bar{y}_{track-total}\| > r$, $r \equiv \sqrt{\frac{T_1}{T \cdot T_2}}$ yields $\dot{J}_{lin+non} < 0$, and then any sphere

$$B_r \equiv \left\{ \begin{bmatrix} \bar{e}_{track} \\ \bar{\eta}_{non} \end{bmatrix} : \|\bar{e}_{track}\|^2 + \|\bar{\eta}_{non}\|^2 \leq r^2 \right\} \quad (A.23)$$

will be a global final attractor of the nonlinear FLMA system with the convergent radius $r \equiv \sqrt{\frac{T_1}{T \cdot T_2}}$.

Next, we will verify the globally exponential stability of the nonlinear FLMA system. Combining (A.17) and (A.19) yields

$$J_{lin+non}(t) \leq J_{lin+non}(t_0) e^{-\frac{T \cdot T_2}{\Delta_{max}}(t-t_0)} + \frac{\Delta_{max} T_1}{T \cdot T_2}, t \geq t_0 \quad (A.24)$$

and

$$\begin{aligned} \Delta_{min} \|\bar{y}_{track-total}\|^2 &\leq J_{lin+non} \leq J_{non}(t_0) e^{-\frac{T \cdot T_2}{\Delta_{max}}(t-t_0)} + \frac{\Delta_{max} T_1}{T \cdot T_2} \\ &\leq \Delta_{max} \|\bar{y}_{track-total}(t_0)\|^2 e^{-\frac{T \cdot T_2}{\Delta_{max}}(t-t_0)} + \frac{\Delta_{max} T_1}{T \cdot T_2} \end{aligned} \quad (A.25)$$

Then

$$\|\bar{y}_{track-total}\|^2 \leq \frac{\Delta_{max}}{\Delta_{min}} \|\bar{y}_{track-total}(t_0)\|^2 e^{-\frac{T \cdot T_2}{\Delta_{max}}(t-t_0)} + \frac{T_1}{T \cdot T_2} \frac{\Delta_{max}}{\Delta_{min}} \quad (A.26)$$

Hence we can achieve the globally exponential stability of the global final attractor.

References

1. S. A. Marinovic, M. T. Torriti and F. A. Cheein, "General dynamic model for skid-steer mobile manipulators with wheel-ground interactions," *IEEE/ASME Trans. Mechatronics*, vol. 22, no. 1, pp. 433–444, Feb. 2017.
2. Z. Li and S. S. Ge, *Fundamentals in modeling and control of mobile manipulators*. Boca Raton, FL, USA: CRC Press, 2013.
3. J. Wu, J. Gao, R. Song, R. Li, Y. Li and L. Jiang, "The design and control of a 3 DOF lower limb rehabilitation robot", *Mechatronics*, vol. 33, pp. 13-22, 2016.

4. X. Wang, H. Zeng and H. Zhou, "A spatial four-link 4R biped walking mechanism," in *2019 IEEE 9th Annual International Conference on CYBER Technology in Automation, Control, and Intelligent Systems*, Suzhou, China, July, 2019, pp. 203-208.
5. M. U. Masood, M. Mujtaba, M. A. Sami, N. Rashid and J. Iqbal, "Design and experimental testing of an in-parallel actuated 3 DOF serial robotic manipulator for unmanned ground vehicle," in *2018 3rd Asia-Pacific Conference on Intelligent Robot Systems (ACIRS)*, Singapore, Singapore, July, 2018, pp. 45-49.
6. F. Leborne, V. Creuze, A. Chemori, L. Brignone and J. Iqbal, "Dynamic modeling and identification of an heterogeneously actuated underwater manipulator arm," in *2018 IEEE International Conference on Robotics and Automation (ICRA)*, Brisbane, Australia, May, 2018, pp. 4955-4960.
7. M. Reyhanoglu, A. van der Schaft, N. H. Mcclamroch and I. Kolmanovsky, "Dynamics and control of a class of underactuated mechanical systems," *IEEE Transactions on Automatic Control*, vol.44, no. 9, pp. 1663 – 1671, 1999.
8. X. Lai, Y. Wang, M. Wu and W. Cao, "Stable Control Strategy for Planar Three-Link Underactuated Mechanical System," *IEEE/ASME Transactions on Mechatronics*, vol. 21, no., 3, pp. 1345 – 1356, 2016.
9. X. Z. Lai, A. C. Zhang, J. H. She, and M. Wu, "Motion control of underactuated three-link gymnast robot based on combination of energy and posture," *IET Control Theory Appl.*, vol. 5, no. 13, pp. 1484–1492, 2011.
10. M. R. Thompson, M. T. Torriti, F. A. Auat Cheeina and G. Troni, "H ∞ -Based Terrain Disturbance Rejection for Hydraulically Actuated Mobile Manipulators With a Nonrigid Link," *IEEE/ASME Transactions on Mechatronics*, vol. 25, no. 5, pp. 2523 - 2533, 2020.
11. S. C. Brown and K. M. Passino, "Intelligent control for an acrobat," *J. Intell. Robot. Syst.*, vol. 18, no. 3, pp. 209 – 248, 1997.
12. X. Z. Lai, A. C. Zhang, J. H. She, and M. Wu, "Motion control of underactuated three-link gymnast robot based on combination of energy and posture," *IET Control Theory Appl.*, vol. 5, no.13, pp. 1484 – 1493, 2011.
13. I. Fantoni, R. Lozano, and M. W. Spong, "Energy-based control of the pendubot," *IEEE Trans. Autom. Control*, vol. 45, no. 4, pp. 725 – 729, 2002.
14. B. Anditio, A. D. Andrini and Y. Y. Nazaruddin, "Integrating PSO Optimized LQR Controller with Virtual Sensor for Quadrotor Position Control," in *2018 IEEE Conference on Control Technology and Applications*, Copenhagen, Denmark, August, 2018, pp. 1603-1607.
15. J. Yang and Z. Ding, "Global output regulation for a class of lower triangular nonlinear systems: A feedback domination approach," *Automatica*, vol.76, pp. 65-69, 2017.
16. J. Wu, H. Zhou, Z. Liu and M. Gu, "Ride comfort optimization via speed planning and preview semi-active suspension control for autonomous vehicles on uneven roads," *IEEE Transactions on Vehicular Technology*, vol. 69, no. 8, pp. 8343-8355, 2020.
17. M. Liu, Y. Li, X. Rong, S. Zhang and Y. Yin, "Semi-Active Suspension Control Based on Deep Reinforcement Learning," *IEEE Access*, vol. 8, pp. 9978 - 9986, 2020.
18. H. Chen, P. Y. Sun and K.-H. Guo, "A multi-objective control design for active suspensions with hard constraints," in *2003 Proc. Amer. Control Conf.*, 2003 pp. 4371–4376.
19. J. S. Lin and C. J. Huang, "Nonlinear backstepping active suspension design applied to a half-car model," *Veh. Syst. Dyn.*, vol. 42, pp. 373–393, 2004.
20. C. Gohrle, A. Schindler, A. Wagner and O. Sawodny, "Design and vehicle implementation of preview active suspension controllers," *IEEE Trans. Control Syst. Technol.*, vol. 22, no. 3, pp. 1135–1142, 2014.
21. L. Tang, D. Ma and J. Zhao, "Adaptive neural control for switched non-linear systems with multiple tracking error constraints," *IET Signal Processing*, vol. 13, no. 3, pp. 330 - 337, 2019.
22. L. Liu, Y. L. Liu, D. Li, S. Tong and Z. Wang, "Barrier Lyapunov function-based adaptive fuzzy FTC for switched systems and its applications to resistance–inductance–capacitance circuit system," *IEEE Transactions on Cybernetics*, vol. 50, no. 8, pp. 3491 - 3502, 2020.
23. R. Cui, C. Yang, Y. Li and S. Sharma, "Adaptive neural network control of AUVs with control input nonlinearities using reinforcement learning," *IEEE Trans. Syst., Man, Cybern., Syst.*, vol. 47, no. 6, pp. 1019–1029, 2017.
24. D. Y. Wang and H. Wang, "Control method of vehicle semi active suspensions based on variable universe fuzzy control," *China Mech. Eng.*, vol. 28, no. 3, pp. 366-372, 2017.

25. H. Li, Y. H. Feng and L. Su, "Vehicle active suspension vibration control based on robust neural network," *Chin. J. Construct. Mach.*, vol. 15, no. 4, pp. 324-337, 2017.
26. Y. Y. Nazaruddin and P. Astuti, "Development of intelligent controller with virtual sensing", *ITB J. Eng. Sci* , vol. 41, no. 1, pp.17-36, 2009.
27. M. Reyhanoglu, A. Schaft, and N. H. Clamroch, " Dynamics and control of a class of underactuated mechanical systems," *IEEE Trans. Autom. Control*. vol. 44, no. 9, pp. 1663 - 1671, 1999.
28. A. D. Luca, R. Mattone, and G. Oriolo, "Stabilization of an underactuated planar 2R manipulator," *Int. J. Robust Nonlinear Control*, vol. 10, no. 4, pp. 181–1812, 2000.
29. T. Yoshikawa, K. Kobayashi, and T. Watanabe, "Design of a desirable trajectory and convergent control for 3-DOF manipulator with a nonholonomic constraint," in *Proc. IEEE Int. Conf. Robot. Autom.*, San Francisco, , USA, 2000, vol. 2, no. 4, pp. 1805–18052.
30. P. Y. Xiong, X. Z. Lai, and M.Wu, "A stable control for second-order nonholonomic planar underactuated mechanical system: Energy attenuation approach," *Int. J. Control*, vol. 91, no. 7, pp. 1630–16302, 2018.
31. S. Zapolsky and E. Drumwright, "Inverse dynamics with rigid contact and friction," *Auton. Robots*, vol. 41, no. 4, pp. 831–8312, 2017.
32. T. Liu, X. Ma, F. Zhu and M. Fadel, "Reduced-Order Feedback Linearization for Independent Torque Control of a Dual Parallel-PMSM system," *IEEE Access*, pp. 1-1, 2021.
33. M. Mehrasa, M. Babaie, M. Sharifzadeh and K. A.Haddad, "An Input-Output Feedback Linearization Control Method Synthesized by Artificial Neural Network (ANN) for Grid-Tied Packed E-Cell Inverter," *IEEE Transactions on Industry Applications*, pp. 1-1, 2021.
34. M. Awais, L. Khan, R. Badar, S. Mumtaz, S. Ahmad and S. Ullah, "Wavelet-Hybridized NeuroFuzzy Feedback Linearization based Control Strategy for PHEVs Charging Station in a Smart Microgrid, " in *2020 International Symposium on Recent Advances in Electrical Engineering & Computer Sciences (RAEE & CS)*, Pakistan, Islamabad, Oct., 2020, pp. 1-6.
35. S. A. Babar, I. Ahmad, I. S. Mughal and S. A. Khan, "Terminal Synergetic and State Feedback Linearization based Controllers for Artificial Pancreas in Type 1 Diabetic Patients," *IEEE Access*, pp. 1-1, 2021.
36. J. Khazaei, Z. Tu, A. Asrari and W. Liu, "Feedback Linearization Control of Converters with LCL Filter For Weak AC Grid Integration," *IEEE Transactions on Power Systems*, pp. 1-1, 2021.
37. R. Marino, W. Respondek and A. J. Van Der Schaft, "Almost disturbance decoupling for single-input single-output nonlinear systems," *IEEE Trans. Automat. Contr.*, vol.34, no. 9, September, pp. 1013-1017, 1989.
38. R. Marino and P. Tomei, "Nonlinear output feedback tracking with almost disturbance decoupling," *IEEE Trans. Automat. Contr.*, vol.44, no. 1, January, pp. 18-28, 1999.
39. A. Isidori, *Nonlinear control system*. New York: Springer Verlag, 1989.
40. H. K. Khalil, *Nonlinear systems*, New Jersey: Prentice-Hall, 1996.
41. H. S. Dhiman and D. Deb, "Fuzzy TOPSIS and fuzzy COPRAS based multi-criteria decision making for hybrid wind farms," *Energy*, vol. 202, pp. 1-10, 117755117755, 2020.

Disclaimer/Publisher's Note: The statements, opinions and data contained in all publications are solely those of the individual author(s) and contributor(s) and not of MDPI and/or the editor(s). MDPI and/or the editor(s) disclaim responsibility for any injury to people or property resulting from any ideas, methods, instructions or products referred to in the content.